UC Davis
UC Davis Electronic Theses and Dissertations

Title

Characterizing Drought-Induced Responses in Grapevine (Vitis) Root Systems

Permalink

https://escholarship.org/uc/item/9p06h92g

Author

Reyes, Clarissa

Publication Date

2021

Peer reviewed|Thesis/dissertation

Characterizing Drought-Induced Responses in Grapevine (*Vitis*) Root Systems

By

CLARISSA REYES
THESIS

Submitted in partial satisfaction of the requirements for the degree of

MASTER OF SCIENCE

in

Horticulture and Agronomy

in the

OFFICE OF GRADUATE STUDIES

of the

UNIVERSITY OF CALIFORNIA

DAVIS

Approved:

_____

M. Andrew Walker, Chair

_____

Elisabeth J. Forrestel

_____

Andrew J. McElrone

Committee in Charge

2021

Table of Contents

List of Figures and Tables

Acknowledgements

Abstract

Water scarcity threatens agricultural production in arid growing regions around the globe, and changing climatic conditions are expected to exacerbate this situation. To optimize production under these conditions, growers require plant materials that better tolerate drought stress to enable conservation techniques like deficit irrigation. To improve drought resistance of rootstocks for use in viticultural production, *Vitis* species originating from arid regions of the southwestern US hold tremendous potential. Several species originate from arid regions suggesting the existence of putative drought resistance traits that could improve grapevine rootstock performance under water limited conditions. In 2019 and 2020, grapevine genotypes *Vitis aestivalis (*accession T52), *Vitis acerifolia* (9018), *Vitis arizonica* (b40-14), *Vitis riparia* (TXNM0821), *Vitis rupestris* (Vru42), *Vitis vulpina* (V57-96) were grown from herbaceous cuttings and subjected to a controlled dry down ("drought") or maintained well-watered. During the controlled dry down, bulk soil moisture (SM) was reduced gradually from 80% w/w to reach a target of 20–30% w/w over ~2 weeks. Treatments were then held for an additional 3-4 weeks. The intended control and drought conditions imposed during the potted vine dry down experiment were evaluated with soil moisture and physiological measurements. Most striking in my research is the discovery that among the six species that were studied, cortical lacuna occurred at lower levels of water stress and more frequently overall in *V. rupestris*; this could help explain variable drought resistance traits among commonly used rootstocks that originate from this and other species. Consistent with expectations, the drought treatment increased root suberization, which reduces fine root conductivity, but did so differentially among the species. *V. riparia* exhibited the highest suberin development under both drought

and control conditions, which is consistent with patterns documented previously for rootstocks with this species parentage. *V. rupestris* had the highest number of root tips of all species, which corresponds to its lowest percent suberization measured from the colored images and indicates production of new growth and active water uptake sites. Characterization of root morphology via image analysis revealed differences in root function among species. Species that exhibited greater transport capacity were *V. acerifolia > V. aestivalis > V. vulpina*, while species with more absorptive capacity were *V. arizonica > V. rupestris > V. riparia*. Overall, this work demonstrated differential responses of diverse *Vitis* species to drought stress with respect to fine root anatomy, root architecture, and implied physiological function.

Introduction

Water scarcity threatens agricultural production in arid growing regions around the globe, and changing climatic conditions are expected to exacerbate this situation (Cook, et al., 2004). Premium viticultural production could be particularly susceptible as it most commonly occurs in growing regions with Mediterranean-type climates, which are characterized by long dry periods during the growing season. To optimize production under these conditions, growers require plant materials that better tolerate drought stress to enable conservation techniques like deficit irrigation. *Vitis* species originating from arid regions of the southwestern US hold tremendous potential for improving drought resistance of rootstocks. Several species originate from arid regions suggesting the existence of putative drought resistance traits that could improve grapevine rootstock performance under water limited conditions.

Drought resistance in cultivated crops can be defined as the ability of a plant to maintain growth, yield, and fruit quality when exposed to periods of water deficit (Blum 2011; Blum, et al., 2015). One fundamental function of a root system is to match canopy water demands necessary to sustain carbon assimilation and plant growth (Kramer & Boyer, 1995). As a result, when crop species experience drought stress, changes to root architecture and allocation patterns can be induced. Commercial grapevine rootstocks are thought to impart drought resistance to grapevine scions by partitioning roots deeper in the soil profile (Padgett-Johnson, et al., 2003) and/or maintaining activity at depth later into the growing season (Alsina, et al., 2011). In woody plants like grapevines, where coarse roots have been defined as >2 mm and usually suberized and fine roots are defined as <2 mm and may or may not be suberized (McCormack, et al., 2015; Comas, et al., 2013), expansive growth of coarse roots is important,

1

but the functionality of fine roots is likely paramount as this portion of the root system

contributes disproportionately to root system water uptake (Queen, 1967; Gambetta, et al.,

2013) and is also vulnerable to hydraulic failure when subjected to drying soil (Cuneo, et al.,

2016). Drought-induced shift in allocation to increase root:shoot ratio is presumably

advantageous because it increases soil water uptake, but at the expense of photosynthetic

carbon gain. Therefore, increased carbon investment in roots comes at a cost to the rest of

plant growth (Ho, et al., 2005). Work is still needed to determine whether inherent differences

and stress-induced changes in the structure and function of root systems play an important role

in differential responses of *Vitis* germplasm to drought.

As the fine roots mature, suberin barriers (e.g., exodermis and endodermis) form

towards the root tip, decreasing the permeability of the tissue and potentially reducing water

loss (i.e., leakiness) from roots to the drying soil (Aroca, et al., 2012; North & Nobel, 1991). The

impacts of suberin on fine root function can be better understood in the context of water

movement across the root cylinder. Water traversing a fine root follows two main pathways:

within the cell walls (apoplastic pathway) and through the symplast (cell-to-cell pathway). The

contribution of each pathway depends on the existing driving force (i.e., water potential

gradient) and the hydraulic properties of the path (Steudle, 2000). A hydrostatic force (i.e.,

negative pressure gradient) resulting from shoot transpiration is the main driver for water

movement into and across roots, and flow under these conditions is dominated by the

apoplastic pathway. Flow in the cell-to-cell pathway is driven mainly by an osmotic gradient

from the soil to the root, and under water deficit this pathway can contribute more to the

movement of water across fine roots (Knipfer & Fricke, 2011). This switch in pathway

contribution has been associated with the development of apoplastic barriers (i.e., suberization of exodermis and endodermis) that force water to cross via the cell-to-cell pathway, and the abundance and activity of aquaporins embedded in cell membranes that increase the efficiency of water moving between cells and alter fine root hydraulic conductivity (Gambetta, et al., 2013; Hachez, et al., 2012). Previous work in the McElrone Lab documented how suberization, aquaporin gene expression, and hydraulic conductivity changed along the length of grapevine fine roots for commercial rootstock 110R (Gambetta, et al., 2013). Additionally, Gambetta, et al. (2012) showed that drought-resistant rootstock 110R had higher inherent aquaporin gene expression under well-watered conditions relative to several rootstocks, and Barrios-Masias, et al. (2015) showed that 110R maintained higher hydraulic conductivity under low soil moisture availability compared to a drought intolerant rootstock, which likely involved slower suberization rates and higher aquaporin activity in young roots. Given that commercial rootstocks were derived from North American *Vitis* species, it is likely that these traits will play an important role in a differential response of the species themselves. The tradeoffs between the earliness of root maturation and decrease in water uptake capacity along the length of young roots may determine the drought resistance potential of native *Vitis* species under agricultural settings.

Cuneo, et al. (2016) showed that cortical lacuna (i.e. air-voids in the cortex resulting from cell tearing) formation is induced in grapevine fine roots as a response to water or osmotic stress. Lacuna formed in fine roots of a commercial grapevine rootstock when it was subjected to mild-moderate stress (-0.5 MPa), and their formation corresponded with plummeting hydraulic conductivity of the fine roots (Cuneo, et al., 2016). More recently, Cuneo, et al. (2021)

found that cortical lacuna formed more rapidly in the drought tolerant rootstock 110R, compared to the drought susceptible rootstock 101-14Mgt. They hypothesized that lacuna formation in 110R helps it to maintain resource distribution to root tips, thus enabling rapid recovery of growth upon rewatering. Work is still needed to evaluate the role of lacuna formation in fine root function across *Vitis* species.

Dr. Walker maintains a germplasm that includes a large collection of rootstock and wild species accessions from arid habitats across the southwestern US, which hold tremendous potential to produce drought resistant rootstocks. My thesis research focused on characterizing the drought response of several *Vitis* species from this collection to gain insight into drought resistance mechanisms and traits important for future commercial rootstock development. This work demonstrated differential responses of grapevine root systems to drought stress with respect to fine root anatomy, root architecture, and implied physiological function.

Materials and Methods

Plant material and growing conditions

In 2019 and 2020, select grapevine genotypes (*Vitis aestivalis*, accession T52; *Vitis acerifolia*, accession 9018; *Vitis arizonica*, accession b40-14; *Vitis riparia*, TXNM0821; *Vitis rupestris*, Vru42; *Vitis vulpina*, V57-96) were grown from herbaceous cuttings from Tyree research vineyard (Davis, CA). The basal node of each cutting was soaked in auxin rooting solution (Earth Science Products), placed in a tray with vermiculite, and maintained in a mist room for approximately 21 days until roots initiated. Cuttings were subsequently potted into two differently sized treepots (Steuwe & Sons). In 2019, treepots measured 12.1 L, 22.8 x 39 cm

(model TP915R) and had additional holes cut for adequate drainage. In 2020, treepots

measured 7.5 L, 19.6 x 31.75 cm. The growth substrate was 50:50 sand:peat over vermiculite at

the bottom of the pot. Plants were watered with Hoagland's solution for 52 days (2019) and

~35 days (2020) to establish growth, and then maintained in a greenhouse at 80% gravimetric

field capacity and with temperatures between 20-28°C. The day-length was on average 14/10 h

for day/night, respectively.

Water potential and gas exchange measurements

A pressure chamber (PMS Instrument Company, Model 1505D) was used to measure

stem water potential. Lights were turned off the evening prior to measuring stem water

potential at predawn (Ψ_{PD}), which was measured between 4 AM and 6 AM before sunrise. Stem

water potential at midday (Ψ_{MD}) was measured between 11 AM and 1 PM. Before

measurements, a fully expanded leaf located 6-8 nodes back from shoot tip was covered with a

Mylar plastic bag for at least 15 min and excised from the petiole using a razor blade.

Subsequently, leaves were excised at the base of the petiole and placed into the pressure

chamber, within a few seconds while still bagged. The chamber was slowly pressurized, and the

pressure was recorded when a water meniscus started to form on the cut petiole surface

(Knipfer, et al., 2019).

Stomatal conductance (g_s) and CO_2 assimilation rate (A) was measured between 11 AM

and 1 PM using an LICOR-6800 gas exchange system (reference CO_2 at 400 ppm, fan speed at

10,000 rpm, temperature at 30°C, and light at 1400 μmol m^{-2} s^{-1}) on leaves similar to those

used for water potential measurements. Intrinsic water-use efficiency (WUE) was calculated by A/g_s (Condon, et al., 2002).

Irrigation treatment

The experimental design included two water treatments, with 5-8 plants per genotype arranged in a randomized complete block design. Plants were either subjected to a controlled dry down ("drought") or maintained irrigated as described above ("control"). During the controlled dry down, bulk soil moisture (SM) was reduced gradually from 80% w/w to reach a target of 20–30% w/w over 12 days (2019) or 14 days (2020). Treatments were then held for an additional 36 (2019) or 26 (2020) days. To account for soil evaporation, each block contained at least one reference pot filled with soil and no plant.

Over the time of the experiment, SM was estimated by measurement of pot mass (Intelligent Weighing Technology, model UFM-B30). Initial pot mass ($m_{pot} = m_{soil} + m_{water} + m_{plastic} + m_{grapevine}$) was measured with the soil at field capacity. $m_{grapevine}$ could not be measured throughout the course of the experiment and was assumed constant over shorter time periods. In practice, pot mass was measured every 2-3 days between 2 PM and 4 PM using a digital balance. Current SM was calculated and water was subsequently added to reach the target soil moisture value: 80% field capacity for controls and eventually down to 30% for drought treatment. To verify soil moisture estimates, soil cores at 10 and 25 cm depths were extracted (containing ~ 10 g of soil) at the end of the dry down period and gravimetric water content (θ) was measured by $(m_{soil-wet} - m_{soil-dry})/m_{soil-dry}$.

Canopy biomass

Lateral shoots were cut from the primary shoot with pruning shears and collected in a Ziploc bag. The primary shoot was cut 5 cm above the soil line, collected in the same Ziploc bag, and weighed for a fresh mass (mass of bag subtracted). In the lab, cut shoots were defoliated. Excised shoots and leaves were transferred to paper bags and dried in a drying oven at 65°C for at least 3 days, then weighed for a dry mass (mass of dried paper bag subtracted).

Root hydraulic conductance

Prior to canopy excision, the soil was saturated to field capacity to release capillary forces within the soil matrix (Knipfer, et al., 2020). After 1 hour to allow for water to disperse through the soil, the canopy was excised ~ 5 cm above the soil surface with pruning shears. A 5 cm piece of silicone tubing was fitted over the stem and sealed by wrapping the bottom end of the tubing with Parafilm. Immediately after this step was completed ($t_{initial}$ = 0 min), root exudate filled the tubing over time. Over approximately 60 min, root exudate was intermittently collected (to prevent exudate overflow from the tubing) using a micropipette and transferred into a pre-weighed 2-ml Eppendorf tube, which was weighed again to determine exudate mass (Mettler Toledo, model MS204DU). The time point of exudate collection was recorded (t_{final}), and Δt was determined by $t_{final} - t_{initial}$. Exudate mass was translated into volume of exudate (ΔV, 1 g = 1 ml H_2O), and the flow rate of exudate was determined by $\Delta V/\Delta t$. Unfortunately, the osmotic potential of the collected exudate was not analyzed in time as the sample became contaminated with fungi for the 2019 experiment, and surprisingly exudate generation in 2020 did not occur in many of the genotypes.

Root biomass

For measurements of root fresh mass, the root system was gently removed from the pot, placed on a fine mesh sieve and massaged to remove bulk soil. Care was taken that fine roots were not removed by soil removal. Root systems were then rinsed in a bucket of water to remove remaining adhering soil and placed into individual Ziploc bags for storage until they could be processed in the lab. After stem diameter was measured and individual roots were excised and scanned, these were combined with the bulk root system and transferred to a paper bag and weighed for a fresh mass (mass of paper bag subtracted). Paper bags containing root systems were dried in a drying oven at 65°C for at least 5 days before obtaining a dry mass (mass of dried paper bag subtracted).

Morphological measurements

Individual roots were excised at the base of root systems taken from the dry down experiment and carefully isolated. Excised roots were placed on the scanner (Epson, Model Expression 12000XL), gently covered with hydrated blotter paper, and scans were taken at photo resolution, 300 dpi (Epson Scan 2 Software). After excised roots were scanned, segments with intact white tips were removed with scissors for anatomical analysis (described below). Excised segments were inserted into a 50-ml Falcon tube and stored in the fridge at 4°C until processed for microscopy.

Binary masks of excised roots were created in Fiji imaging- processing software (www.fiji.sc, IMAGEJ) by "Splitting Channels" of colored images and thresholding blue and red channels individually to value of 75, and Image Calculator was used to add the two binary

images. To measure suberized and unsuberized regions of excised roots, white regions of excised roots were extracted by "Splitting Channels" of colored images, thresholding the red channel to a value of 75, and inverting the values of the resulting binary image to create a separate mask. "Image Calculator" was used to subtract the mask of white region from the whole root system mask to calculate the percent of the root system's suberized and unsuberized regions.

To measure root diameter, length, surface area, and number of root tips, binary masks were despeckled to remove noise in ImageJ and subsequently processed with RhizoVision Explorer (Seethepalli & York, 2020). Images were processed via Batch Analysis with the following parameters: Broken roots analysis, 300 dpi, edge smoothing=1; Root pruning=1, root diameter range 1 = 0-0.5 mm, range 2 = 0.5-1 mm, range 3 = 1-3 mm, range 4 = 3 mm and above. Images of excised roots color-coded by root size diameter were produced by RhizoVision Explorer with medial axis width=3.

Anatomy

Free-hand cross sections were prepared using a fresh razor blade at 6-8 cm from the root tip. Sections were prepared within 5 days following sample collection, stained for at least 30 min with 0.05% Toluidine blue, and subsequently rinsed with distilled water. Sections were mounted on a glass slide and observed within 2 h after preparation using a microscope (LEICA, Model DM4000 B LED) equipped with a digital camera (LEICA, Model DC7000T). Stained sections were viewed under brightfield to investigate structural integrity of the cortex, and also viewed under fluorescence light mode (excitation range violet/blue, excitation filter BP 436/20,

dichromatic mirror 455, and suppression filter BP 480/30). The bright blue fluorescence signal

emitted from sections indicated the deposition of lignin/suberin (including Casparian bands) in

the endodermis.

Black and white 32-bit microCT images (imaging method described below) were

analyzed in Fiji and measured with polygon drawing tools to determine tissue areas. Images

were thresholded and the "Analyze particles" tool was used to determine intracellular airspace.

Lacuna were determined by discluding intracellular airspace particles with circularity of 0.9-

1.00.

Imaging

Potted vines and root chambers were transported from UC Davis campus to the

Advanced Light Source (ALS) at Lawrence Berkeley National Lab in Berkeley, CA. Leaf water

potential was measured prior to root excision. The root chambers were unclipped and roots

were excised 6-8 cm back from root tips. For root segments that were extracted from soil,

grapevines were carefully removed from pots over a secondary container to catch loose soil.

Root segments were excised 6-8 cm back from root tips, and grapevine and associated soil was

returned to the pot. All excised root segments were sealed within high temperature kapton

tape (ULINE), stabilized in a pipette tip, and mounted into a drill chuck. X-ray imaging of root

tissue was performed at ALS beamline 8.3.2. Plant tissue was imaged with 23 keV synchrotron

X-ray beam and processed by with reconstruction methods described by Knipfer, et al. (2020).

Root chambers

Blotter assay root chambers were constructed similar to Fort, et al. (2017) to evaluate consistency of root anatomy under varied growing conditions (i.e. could a simple and easily harvestable assay reveal similar information to vines potted in soil?). Custom 8"x12" root chambers were constructed from common pegboard (Home Depot), 0.125" reticulated polyurethane foam (United States Plastic Corporation), and blue germination blotter paper (Seedburo Equipment Company). Cuttings were placed between two sheets of hydrated blotter paper sandwiched with foam and pegboard on both sides, and clipped closed with binder clips, based on rhizotron design by Fort, et al. (2017). Each chamber was positioned vertically and irrigated with one drip emitter (Rainbird) at 6 AM, 12 PM and 6 PM for 20 min periods to maintain watered conditions. Chambers were checked weekly for root growth and harvested between 22-40 days for digital camera and microCT images (Figure 24).

Data analysis

Data were analyzed and graphs were generated using Rstudio (RStudio Team, 2020). For main factors "species" and "treatment", analysis of variance (ANOVA) was performed to determine P values for each parameter. Post-hoc analysis was performed using least square means to generate pair-wise comparisons of species within treatment and comparisons between treatments. P values were adjusted using the Tukey method.

Results

Harvest variables

The intended control and drought conditions imposed during the potted vine dry down experiment were evaluated with soil moisture and physiological measurements. Drought treatments significantly reduced soil moisture for all species with some variability amongst species and at different depths (Figure 1 & Figure 2, Table 1 & Table 2). *V. arizonica* had the lowest average soil moisture values for all but one of the samples. Water potential measurements reflected the water stress imposed by the drought treatment with most of the species exhibiting a significant drop in the later stages of the experiment (Figure 3 & Figure 4). In both years, treatment had minimal effect on midday water potentials for *V. riparia* and *V. vulpina,* possibly due to varied daily water use patterns in these species.

Cell expansion and plant growth are directly dependent on turgor and are typically one of the earliest indicators of water stress in plants. In these potted experiments, canopy growth was consistently reduced by the drought treatment, but root response was variable. Drought treatments significantly reduced canopy biomass for all species, with *V. acerifolia*, *V. arizonica*, and *V. rupestris* showing the greatest reductions between control and drought in both years (Figure 5). Root biomass varied across the years: no significant treatment effect was observed in 2019 root biomass, but 2020 root biomass was significantly reduced in all species by the drought treatment (Figure 6), with *V. aestivalis, V. arizonica*, and *V. rupestris* showing the greatest reductions. While reduced canopy growth provides a clear indication of drought stress, root:shoot ratio serves as a useful parameter for assessing carbon allocation. This is particularly

relevant to grapevines, where canopy and berry production are considerably affected by water deficit. In control conditions, all species had root:shoot ratios <1, and therefore more biomass allocated to their canopies. However, in drought conditions, *V. acerifolia, V. aestivalis, V. rupestris*, and *V. vulpina* all exhibited root:shoot ratios >1, indicating more biomass allocation to roots over canopy (Figure 7). Stem diameter (measured only in 2020) for all species were reduced by drought treatment, corresponding to reduced canopy and root biomass, with significant drought-induced shrinkage in *V. aestivalis*, *V. arizonica*, and *V. rupestris* (Figure 8).

Hydraulic conductivity

Root hydraulic conductivity provides a measure to understand water uptake mechanisms from the soil through the plant. In 2019, root exudate flow rate (Figure 9) and exudate normalized for root system biomass (Figure 10) was collected, and both were significantly reduced by drought treatment in all species. *V. aestivalis, V. arizonica* and *V. rupestris* showed the largest drop in response to the drought treatment. In 2020, root exudate measurements were attempted but did not produce measurable amounts of exudate.

Suberin commonly increases in roots as they mature and in response to drought stress. It acts as a barrier to apoplastic water flow, and therefore, affects permeability of the root cylinder. Suberized regions of excised roots were estimated via root image thresholding, with drought-treated grapevines exhibiting significantly higher suberization (Figure 11). In both treatments, *V. rupestris* exhibited the least amount of suberization and *V. riparia* exhibited the most. Suberized regions at a cellular level are visualized by faint fluorescent bands at the exodermis as seen in fine root cross-sections (Figure 12). Root cross-sections were taken 6-8 cm

back from the root tip to standardize developmental stage, but cross-sections for *V. aestivalis* and *V. rupestris* were apparently more developmentally advanced compared to the other species based on xylem formation. In these roots, suberin can be observed more clearly at the exodermis, as well as in the endodermis.

Root anatomical traits also contribute to root hydraulic conductivity, affecting resistance to water flow from soil to xylem transport. Root area, percent of root cortex, and lacuna can all affect the apoplastic flow of water prior to crossing the Casparian strip at the endodermis. Root cross-sectional area measured 6-8 cm back from the root tip in control grapevines varied in each species and by treatment (Figure 13), yet cortical area was consistent all grapevines (84-88%) (Figure 14). In 2020, lacuna were quantified from microCT scans (Figure 12, top row) for fine roots sampled from potted plants at Day 16 of the gradual dry down, two days after treatment reached its target soil moisture for the drought treatment. They were also evaluated in hand-sectioned roots collected from harvested root systems after the drought treatment continued for four additional weeks. Lacuna, reported as a percent of cortex area, was between 0.48-3.59% for all species except *V. rupestris,* and significantly higher in drought-treated plants relative to controls. In *V. rupestris,* lacuna covered 11% of cortical area in control vines and 22% of cortical area in drought-treated vines (Figure 15); this response was consistent across time and obvious in both microCT images and light microscopy sections.

Root architecture

Root architecture can provide information regarding allocation patterns, rooting distribution in the soil profile, and functionality of different portions of the root system.

Individual primary roots and their connected branched roots were excised from whole root systems, measured for root length and diameter, from which surface area was extrapolated, and number of root tips (Figure 16, Table 3). Species showed significant differences from one another in total root length and total surface area despite no significant treatment effects, with *V. acerifolia* reduced relative to other species (Figure 17 & Figure 18). Number of root tips provides a proxy for active growth or uptake sites. While there was also no treatment effect for this variable across species, *V. acerifolia* had the least number of root tips and *V. rupestris* had the greatest (Figure 19), which is apparent in the representative scans of excised roots (Figure 16).

Roots were then classified into diameter size ranges as an approximation of root order where <0.5 mm = 1st order, 0.5-1 mm = 2nd order, and >1 mm = 3rd order. Root distribution based on size class was reported as a percentage of total length (Figure 20) and surface area (Figure 21). When considering root length of the different size classes, only roots 0.5-1 mm were significantly affected by treatment, which increased with drought in all species. For <0.5 mm roots, *V. acerifolia* had the lowest total root length, while *V. vulpina* had the most. For 0.5-1 mm roots, there was no significant difference among species. For >1 mm roots, *V. arizonica* had the least length, while *V. acerifolia* had the most. When considering root surface area, there were no significant differences by treatment or among species in <0.5 mm roots. For 0.5-1 mm roots, surface area increased in drought treatments in all species. For >1 mm roots, surface area did not differ by treatments, but *V. riparia* had the least surface area and *V. vulpina* had the most.

Roots sizes were additionally assigned function based on diameter: <1 mm = absorptive and >1 mm = transport. When classified this way, there was no difference in treatment, but with respect to root length, species ranked from lowest to highest transport roots: *V. arizonica < V. riparia < V. rupestris < V. vulpina < V. aestivalis < V. acerifolia* (Figure 22). With respect to surface area, there was no difference in drought treatment, and species ranked from lowest to highest absorptive roots: *V. aestivalis < V. acerifolia < V. vulpina < V. riparia < V. rupestris < V. arizonica* (Figure 23).

Discussion

Drought resistance is a broad term that can occur through several mechanisms, including drought tolerance, which enable a plant to maintain function at low water potential, and/or dehydration avoidance, which limit loss or increase uptake of water (Bodner, et al., 2015). In my thesis research, I have identified grapevine root characteristics that differ among species at various levels of water deficit and speak to strategies of stress avoidance via osmotic regulation and root-soil isolation, and dehydration avoidance via root exploration. Most striking in my research is the discovery that among the six species that were studied, cortical lacuna occurred at lower levels of water stress and more frequently overall in *V. rupestris*. Given that cortical lacuna impacts axial and radial water transport across the root by disrupting apoplastic flow across the cortex, and *V. rupestris* is a parent in commonly used rootstocks, this provides critical insight to hydraulic differences previously found by Cuneo, et al. (2021) in 101-14Mgt (*V. rupestris* x *V. riparia)* and 110R (*V. berlandieri* x *V. rupestris*), and invites further exploration of how species interaction with *V. rupestris* affects lacuna formation at variable levels of water stress, as well as potential recovery of hydraulic conductivity thereafter. Additionally,

characterization of root morphology via image analysis revealed differences in root function among species. Species that showed more transport capacity were *V. acerifolia > V. aestivalis > V. vulpina*, while species with more absorptive capacity were *V. arizonica > V. rupestris > V. riparia*.

In the dry down experiment, soil moisture values effectively confirmed the drought treatment. Many physiological measurements were collected, including pre-dawn and midday water potentials, and gas exchange measurements, but not all were reported here. *V. arizonica* showed consistently low gravimetric water content for all regions, treatments, and years, which might correspond to higher hydraulic conductivity by the roots, transpiration through the canopy, or combined effect of both (Padgett-Johnson, et al., 2003; Knipfer, et al., 2015). Closer evaluation of gas exchange measurements that were taken, but not included here is necessary to determine an effect of transpiration on soil moisture as a function of water uptake.

Water potential patterns of all species were consistent in both years, with *V. riparia* and *V. vulpina* showing minimal change in water potential over the time of the experiment. *V. riparia* and *V. vulpina* maintained high water status despite water deficit, while *V. aestivalis, V. acerifolia, V. arizonica,* and *V. rupestris* showed significant drops in water potential under water deficit, with *V. rupestris* exhibiting the greatest response. A binary categorization to describe if a plant maintains its water status between droughted and well-watered conditions--isohydric if it does, anisohydric if it does not—is commonly used in viticultural literature. Levin, et al. (2020) recently analyzed the physiological response of numerous *Vitis vinifera* varieties to drought stress and evaluated responses in relation to the iso- vs. anisohydric condition; they found that this binary categorization oversimplifies the response of grapevines varieties to drought stress.

Further evaluation of relationships between predawn and midday water potentials, and stomatal conductance over the course of the dry down is necessary to classify the species in terms of iso/anisohydric behaviors.

Growth and expansion of tissues are one of the most sensitive indicators of drought-induced water stress in grapevines. Non-stressed vines that are actively growing usually have long tendrils that extend past the shoot tip. Under mild water stress, turgor and relative water content start to decrease in grapevine cells, which results in reduced cell division and expansion, and ultimately reduced shoot tip and tendril growth. In 2019, canopy biomass reduction occurred to a much lesser degree than in 2020. A possible explanation for less biomass reduction in 2019 is that grapevine establishment in experimental pots prior to initiating treatment was 52 days, therefore providing substantial initial biomass, whereas grapevine establishment in experimental pots for 2020 was ~35 days. Nevertheless, *V. acerifolia, V. arizonica,* and *V. rupestris* showed the greatest canopy reduction under drought in both years, indicating some drought-susceptible canopy response in these species.

In root systems, water deficit leads to less growth due to a loss of cell turgor and modified allocations towards root growth to increase water uptake area (Lovisolo, et al., 2010). In 2019, drought effects on root biomass were not significant and low root:shoot ratios were driven by large canopies. In 2020, all species exhibited a reduction in root biomass due to drought, corresponding to reduced canopy biomass, though to a lesser degree. All root:shoot ratios were higher under drought relative to control, indicating a shift in carbon allocation to roots to increase the absorptive root surface and decrease water loss by the canopy. This strategy is apparent in the high root:shoot ratios in drought-treated *V. acerifolia*, *V. aestivalis*,

and *V. vulpina*, which were driven by considerably small and dried canopies*. On the other hand, *V. arizonica* exhibited the largest canopies and smallest root systems of the species, with little root:shoot variability from treatment, suggesting a growth strategy with higher carbon allocation towards canopy regardless of water availability. This allocation pattern could further explain the lower soil moisture and water potentials under drought stress in *V. arizonica*.

Stem diameter responds to water deficit, as reduced cell turgor causes shrinkage and stem and xylem cells responsible for water storage and transport release water at lower water potential (Knipfer, et al., 2019; Skelton, 2020). The significant reductions in *V. aestivalis*, *V. arizonica*, and *V. rupestris* stem diameter reflect the canopy response, and suggest less water transport to the canopy under drought conditions.

Differences in root hydraulic conductivity across rootstocks in woody species has been found to be influenced by localization of suberized structures, aquaporin gene expression (Gambetta, et al., 2013), cortical lacuna (Cuneo, et al., 2016), and osmotic regulation (Knipfer, et al., 2020). This study intended to elucidate the driving forces of water uptake across fine roots in different species, but without osmotic measurements in 2019, they could not be determined. Analysis of solutes in exudate would have enabled a calculation for the osmotic component of water potential and how it changes with water deficit, with the possibility to compare among species. Where some measurements were successfully measured, the greatest reduction in flow rate and g exudate/g biomass occurred in *V. acerifolia, V. arizonica,* and *V. rupestris.* Unsurprisingly, this corresponds to the species in which the greatest reduction of root biomass was observed, as flow is limited by the available root surface uptake area.

Exudate measurements were attempted in the 2020 dry down but did not produce volumes large enough to measure in replicate. Nobel & Cui (1992) discussed how in drying soils, water movement is mainly controlled by the root-air gap between a root and its media. The lack of exudate in both control and drought treatments might speak to specific media characteristics that maintain a high water potential (Nobel & Cui, 1992) and, without the driving force of a transpiring canopy, cannot be overcome. When exudate was not produced by the method that was successfully applied by Barrios-Masias, et al. (2015), Knipfer, et al. (2019), and in the 2019 dry down, the period of saturation time prior to canopy excision was increased. Even with saturation periods of 1-2 hours, minimal exudate was produced among all species and treatments. Further method development in different media and with variable saturation periods might be necessary to reliably use this method to measure hydraulic conductivity and driving forces.

Suberization is known to increase with drought stress in the fine roots of grapevines (Barrios-Masias, et al., 2016; Cuneo, et al., 2020). This experiment showed higher suberization in all species due to drought. *V. riparia* roots were the most suberized and *V. rupestris* the least in both treatments. Previous work by Barrios-Masias, et al. (2015) and Cuneo, et al. (2016) showed that grapevine rootstocks differ in suberization responses to drought; in both studies the rootstock with *V. riparia* parentage exhibited more suberization consistent with the findings shown here. Given characterization of suberin development with root development by Gambetta, et al. (2013), greater suberization indicates more developmentally mature root zones in drought-treated plants. In a comparison of species, significantly less suberized area in *V. rupestris* could suggest more active growth and water uptake regions relative to *V. riparia*,

which enable the former to utilize water upon rewatering after drought. This is also consistent with the idea that lacuna formation disintegrates the fine root cells and helps to assure resources for the root tips.

Fine root cross-sectional area was measured because hydraulic conductivity is affected by both radial resistance across the root cortex and surface area that is in contact with soil (Huang & Eissenstat, 2000; Rieger & Litvin, 1999). At the sampling region of 6-8 cm from the root tip, where the exodermis has not yet developed suberin, and if the cortex is intact, a model of uniform resistance applies to water flow across the root. Therefore, in all species where root area and cortical thickness remain constant in control and drought treatments, water permeability should not differ based on these two variables. However, hydraulic conductivity can still be impacted by other variables, such as number of water transport channels, drought-induced chemical signaling, or other forms of resistance (Steudle & Peterson, 1998). An example of such is the occurrence of drought-induced intracellular airspace, i.e. lacuna, within the cortex that can disrupt radial flow, which has been found across several species (North & Nobel, 1991; Yang, et al., 2012; Zhu, et. al, 2010; Cardoso, et al., 2020; Cuneo, et al., 2016). In this study, *V. rupestris* is the only species to exhibit significant lacuna formation in control and drought conditions. Previously, Cuneo, et al. (2021) observed lacuna formation in grapevine rootstocks 110R and 101-14 at different severities of drought stress, with the hypothesis that lacuna functions as a mechanism to reduce respiratory demand of root tissue in times of water deficit. Given that *V. rupestris* is a parent in both rootstocks, variable susceptibility to lacuna formation might be attributed to the other parents. Interactions with other species should be explored to determine if *V. rupestris* is the ultimate source of this lacuna susceptibility trait.

Bartlett, McElrone, et al. (unpublished data) have recently found that commercial rootstocks with *V. rupestris* parentage all showed susceptibility to form lacuna, while those without this species as a parent lacked this trait under control and droughted conditions. It is also worthy to note that lacuna is apparent in hand-sectioned slices and in an early maturation stage, which can enable quick and low-cost characterization of rootstocks for this anatomical feature.

The architecture of roots in soil can provide insight to how a plant optimizes uptake of available water as a mechanism of drought avoidance. In non-irrigated conditions or in times of drought, plants with root systems that extend many lateral roots at a shallow depth will access water differently than root system with long, deep roots (Bodner, et al., 2015). When evaluating root length and surface area (calculated from length and diameter) via image analysis, no treatment effect was observed, but there were differences among species. *V. vulpina* exhibited significantly longer total root length from *V. aestivalis*, and significantly more total surface area than *V. acerifolia*, suggesting than *V. vulpina* might have a more explorative (expansive) root system to access water than other species.

Studies have now shown that due to variability across species, root classification by order is more informative than classification by root size (Lavely, et al., 2020). Using intact root scans to evaluate root morphology provides a method to refer to the original structure of the root system that is impossible to glean when root systems are deconstructed into piece-wise cutting for scanning. Using RhizoVision Explorer, roots were grouped by diameter in ranges that approximated root order to enable characterization of root systems across *Vitis* species related to function. Transport roots represent higher order roots that provide structure and transport and are associated with more developed anatomy and larger diameter. Absorptive fine roots

represent distal roots that facilitate resource acquisition, and are associated with root turnover, respiration, nitrogen content, and mycorrhizal colonization (McCormack, et al., 2015). Length and surface area were measured to speak to these transport and absorptive function, respectively. For both length and surface area, 2nd order roots did not differ among species, leading 3rd order roots to drive species differences in transport function, and 1st order roots to drive differences in absorptive function. *V. acerifolia* had the longest length of transport roots, suggesting an improved ability to reach water in deeper soil than the other species. *V. arizonica* had the greatest surface area of absorptive roots of all species, suggesting a higher capacity to uptake water where it is readily available. *V. rupestris* had the highest number of root tips of all species, which corresponds to its low percent suberization measured from the colored images and indicates production of new, active growth and water uptake sites. However, *V. rupestris* had a similar percentage of absorptive and transport roots, so it is difficult to determine how the new growth may function.

Given unique management to match the environmental conditions of individual vineyard systems, it is important to select rootstock characteristics that will address specific irrigation, soil characteristics, and rainfall/dry seasons of a system. Grapevines that grow on low water storage soils or in irrigated systems would benefit from root systems with more absorptive roots (i.e., shallow architecture with high density of low order roots) whereas grapevines that grow soils with water availability at depth or in rainfed systems would benefit root systems with more transport roots (i.e., long-root architecture with high frequency of higher order roots). However, these system characteristics are likely to change seasonally and

with vineyard age. Work is still needed to determine genotype by environment by management

interactions for current and future rootstock materials.
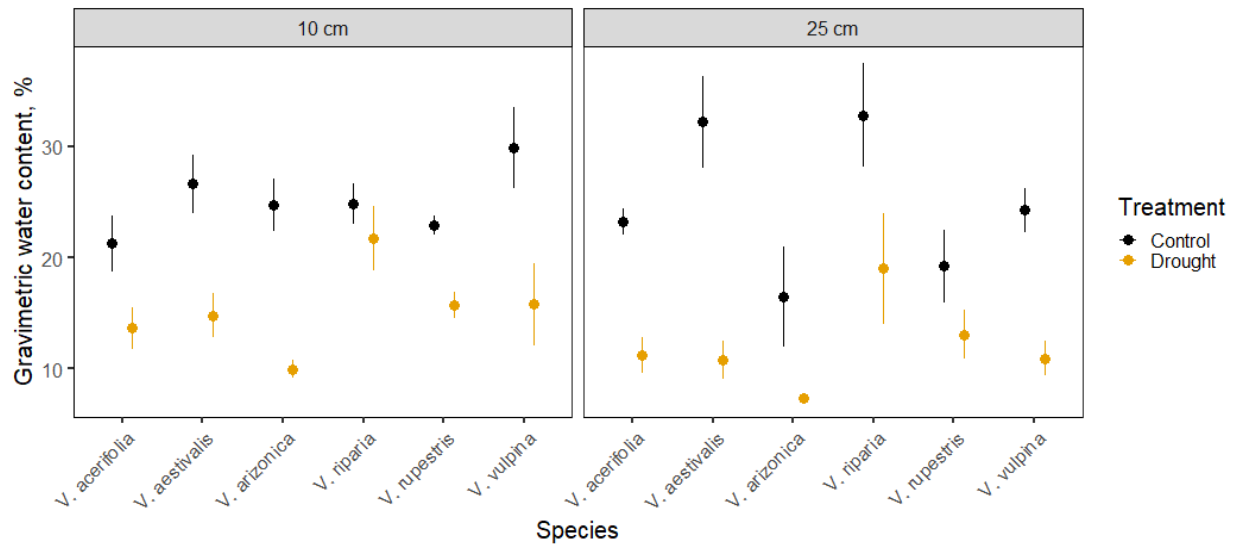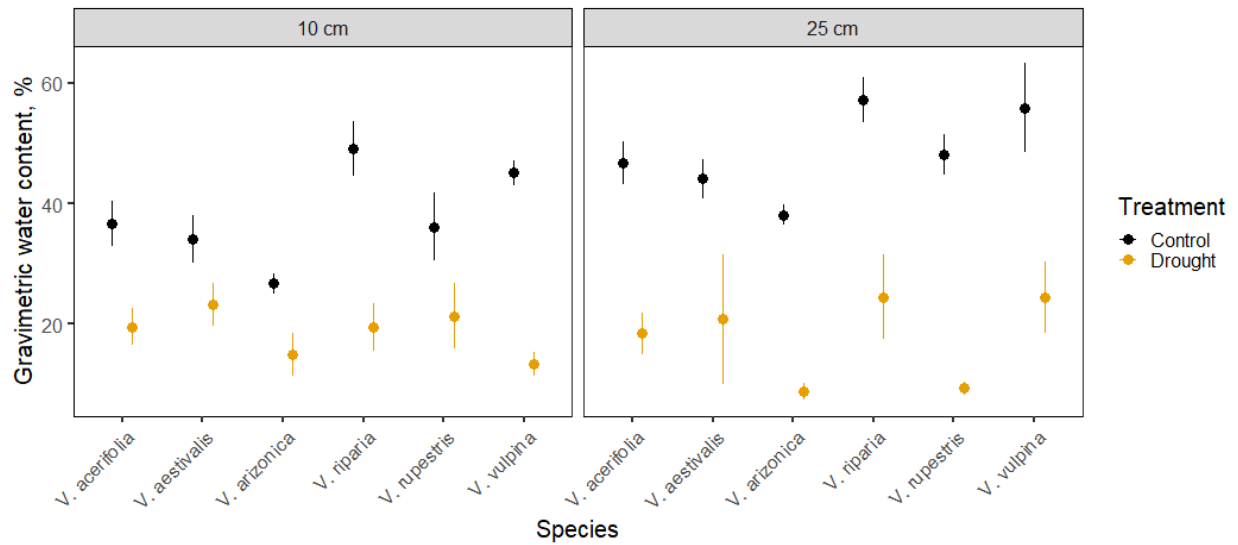
Figures

Harvest variables

Figure 1. 2019 Soil Gravimetric Water Content.
Soil gravimetric water content was measured at two depths, 10 cm (top) and 25 cm (bottom). Each point represents the mean of 4 or more soil samples. Mean values and error bars correspond to data shown in Table 1. ANOVA results: Drought effect (F= 105.937, p= < 2e-16); Species effect (F= 6.406, p= 2.43e-05); Region: (F= 3.453, p= 0.0655); Drought X Species effect (F= 1.877, p= 0.1029), Drought X Region (F= 1.312, p= 0.2542); Species X Region: (F= 1.494, p= 0.1963); Drought X Species X Region (F= 1.447, p= 0.2119).

Figure 2. 2020 Soil Gravimetric Water Content.
Soil gravimetric water content was measured at two depths, 10 cm (top) and 25 cm (bottom). Each point represents the mean of 4 or more soil samples. Mean values and error bars correspond to data shown in Table 2Table 1. ANOVA results: Drought effect (F=172.825, p= < 2e-16); Species effect (F= 8.6257, p= 1.37e-06); Region: (F= 8.042, p= 0.00575); Drought X Species effect (F= 1.491, p= 0.20176); Drought X Region (F= 6.377, p= 0.01349); Species X Region: (F= 0.884, p= 0.49598); Drought X Species X Region (F= 0.956, p= 0.44946).
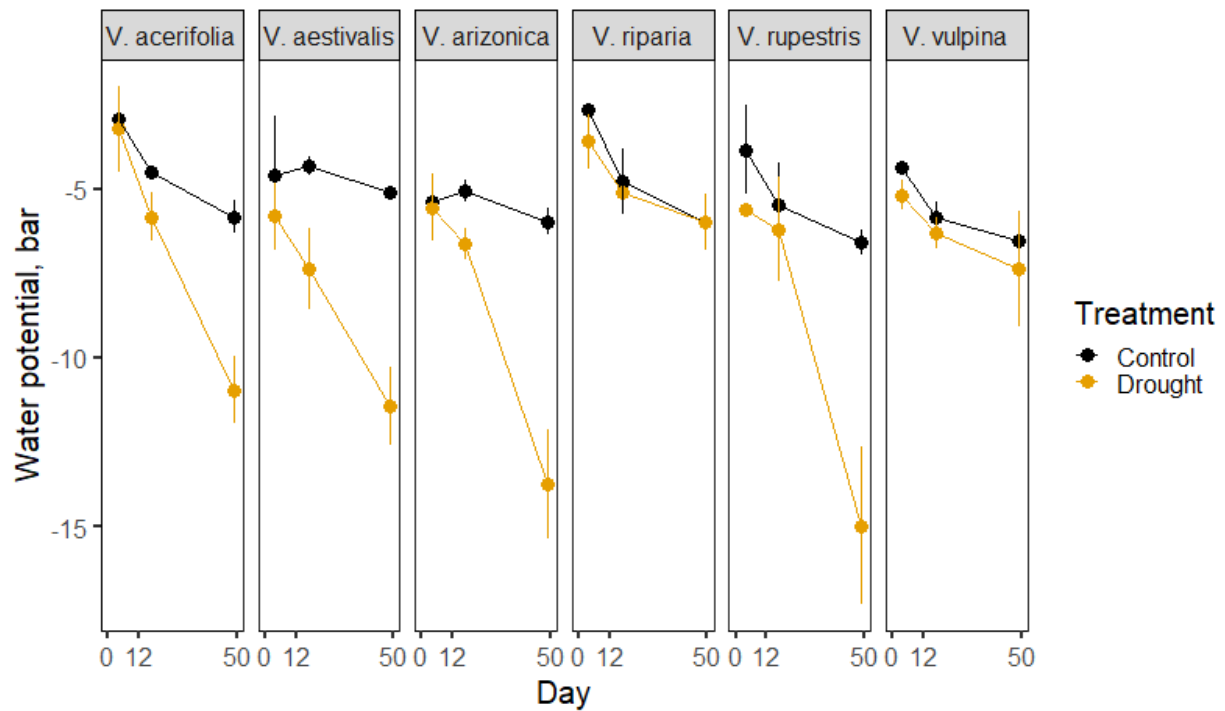
Figure 3. 2019 Midday Stem Water Potential Over Time.
Midday stem water potential was measured over the duration of the experiment to estimate plant water status. Each point represents the mean of 3 or more grapevines. Day 12 marks the beginning of Drought treatment hold. Drought-treated grapevines show reduced water potentials relative to control.
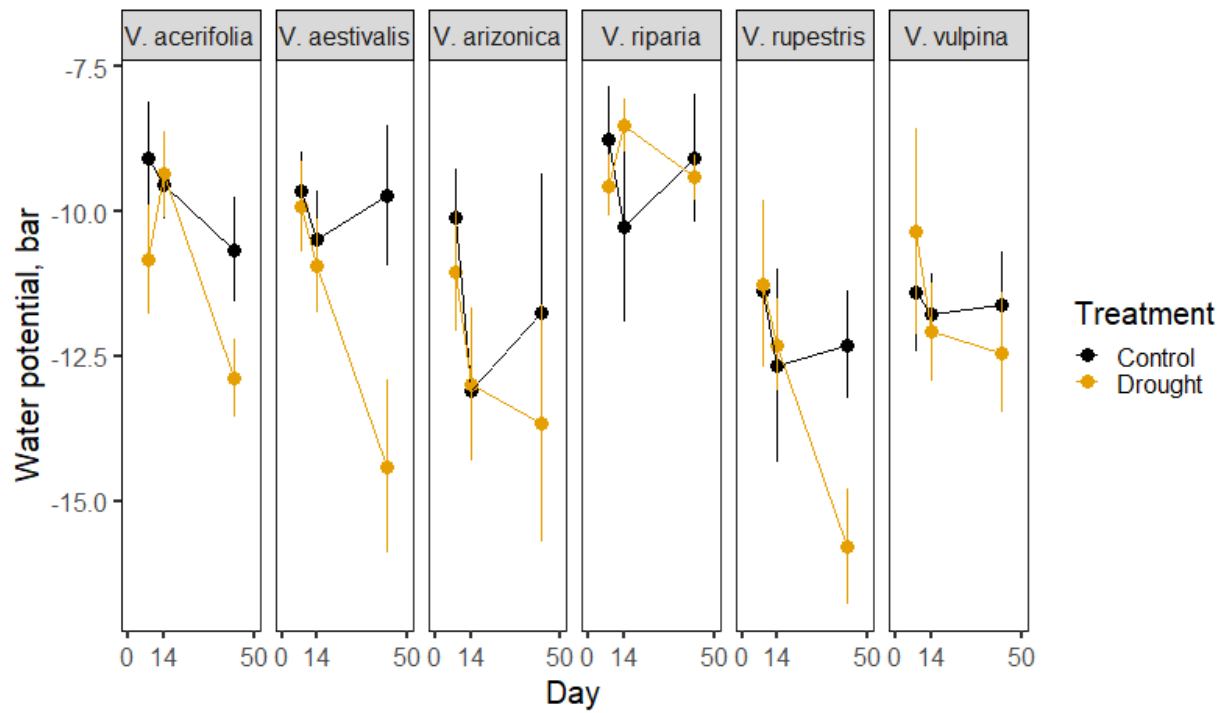
Figure 4. 2020 Midday Stem Water Potential Over Time.
Midday stem water potential was measured to estimate soil water status over the duration of the experiment to estimate plant water status. Each point represents the mean of 4 or more grapevines. Day 14 marks the beginning of Drought treatment hold.
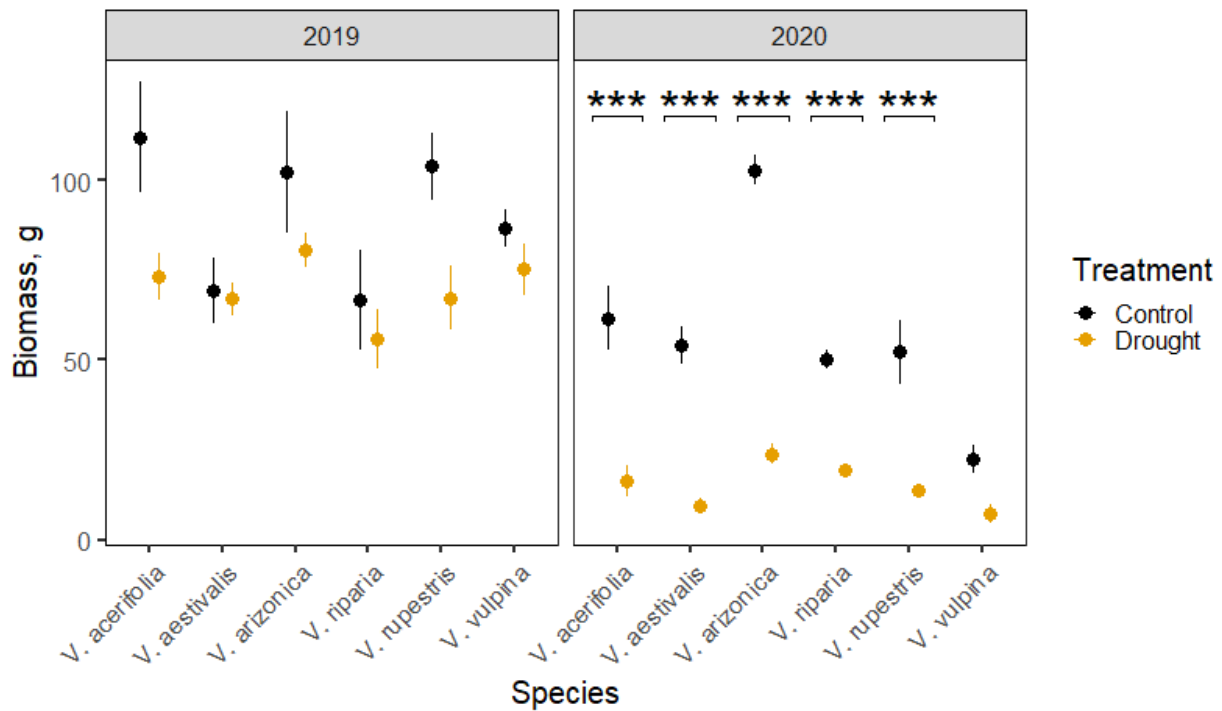
Figure 5. Dry Canopy Biomass from 2019 and 2020 Dry Downs.
Canopies were excised 3 cm from the soil line, dried and weighed to measure biomass. Each point represents the mean of 4 or more grapevines. Bars represent standard error of the mean. Mean values and error bars correspond to data shown in Table 1 & Table 2. 2019 ANOVA results: Drought effect (F= 10.767, p= 0.00185); Species effect (F= 3.080, p= 0.01649); Drought X Species effect (F= 1.044, p= 0.40184). 2020 ANOVA results: Drought effect (F= 217.154, p= < 2e-16); Species effect (F= 19.566, p= 1.16e-10); Drought X Species effect (F= 8.963, p= 4.24e-06). Asterisks indicate post-hoc analysis of species-treatment interaction, if statistically significant: ***p < .001.
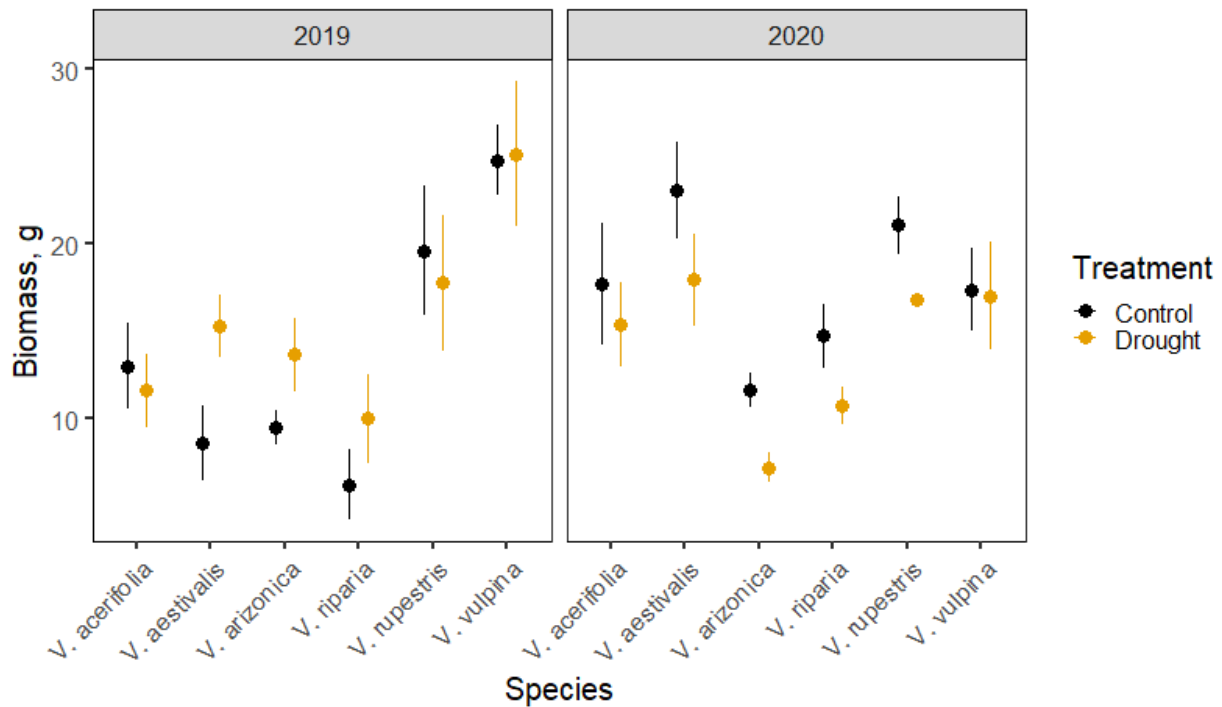
Figure 6. Dry Root System Biomass from 2019 and 2020 Dry Downs.
Root systems were washed of soil, dried and weighed to measure biomass. Each point represents the mean of 4 or more grapevines. Bars represent standard error of the mean. Mean values and error bars correspond to data shown in Table 1 & Table 2. 2019 ANOVA results: Drought effect (F= 1.927, p= 0.171); Species effect (F= 11.401, p= 1.19e-07); Drought X Species effect (F= 0.824, p= 0.537). 2020 ANOVA results: Drought effect (F= 9.312, p= 0.00377); Species effect (F= 7.816, p=2.17e-05); Drought X Species effect (F= 0.491, p= .78139).
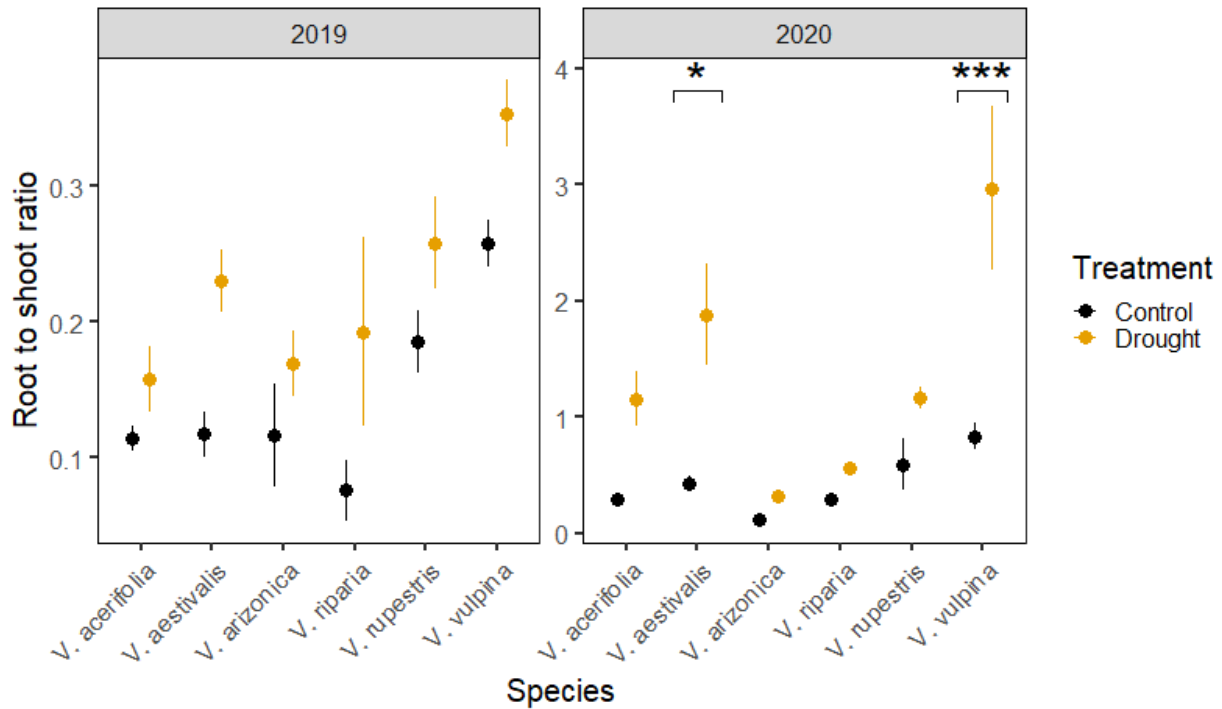
Figure 7. Root:shoot Ratio of Dried Biomass from 2019 and 2020 Dry Downs.
Root:shoot ratio was calculated from dividing dried biomass values. Each point represents the mean of 4 or more grapevines. Bars represent standard error of the mean. Mean values and error bars correspond to data shown in Table 1 & Table 2. 2019 ANOVA results: Drought effect (F= 23.878, p= 1.06e-05); Species effect (F= 11.745, p= 1.40e-07); Drought X Species effect (F= 0.565, p= 0.726). 2020 ANOVA results: Drought effect (F= 39.169, p= 1.09e-07); Species effect (F= 10.922, p= 5.20e-07); Drought X Species effect (F= 4.297, p= 0.00267). Asterisks indicate post-hoc analysis, if statistically significant: *p <0.05, ***p < .001.
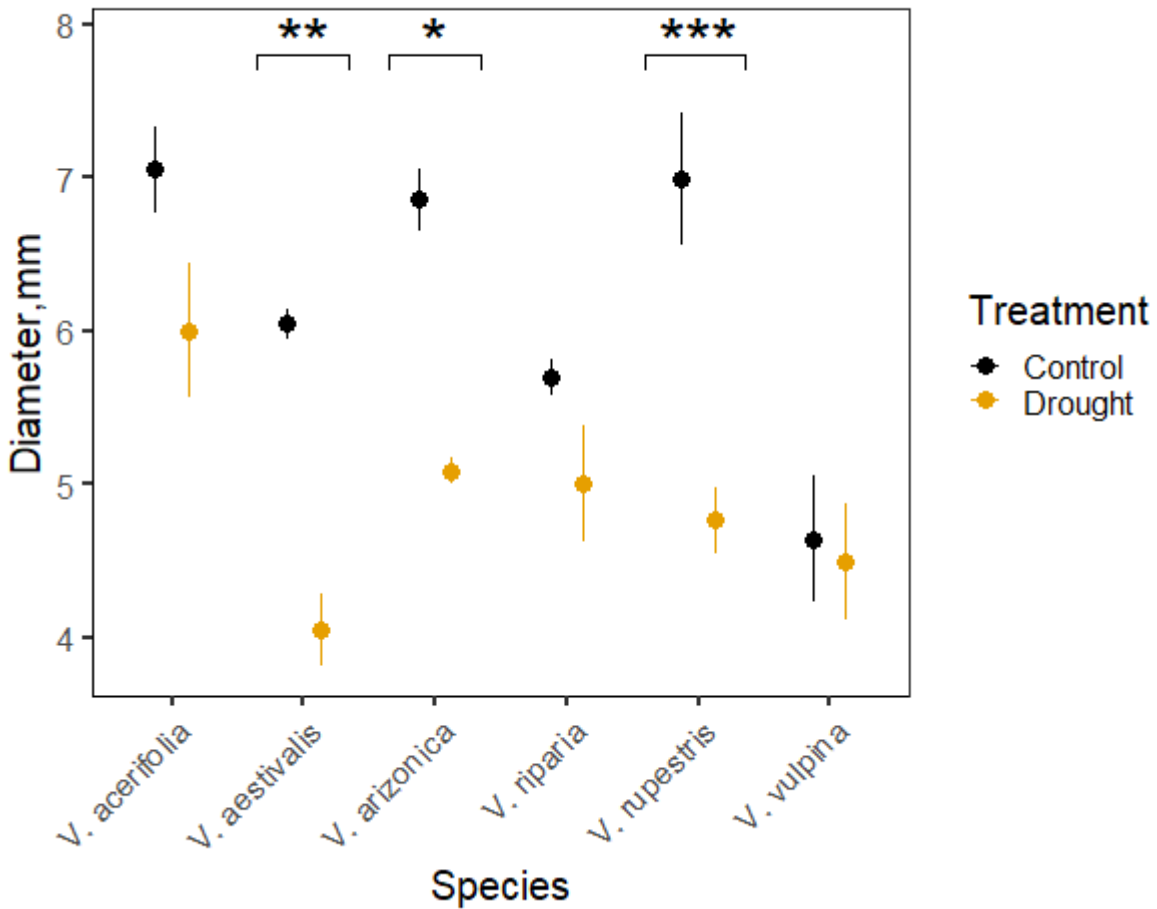
Figure 8. Stem Diameter from 2020 Dry Down.
Hydrated stem diameter was measured in 2020 potted grapevine experiment at harvest. Each point represents the mean of 4 or more grapevines. Bars represent standard error of the mean. Mean values and error bars correspond to data shown in Table 1. ANOVA results: Drought effect (F= 56.209, p=3.84e-09); Species effect (F=11.745, p=5.04e-07); Drought X Species effect (F=3.775, p=0.0068). Asterisks indicate post-hoc analysis of treatment-species interaction, if statistically significant: *p <0.05, **p<0.01, ***p < .001.
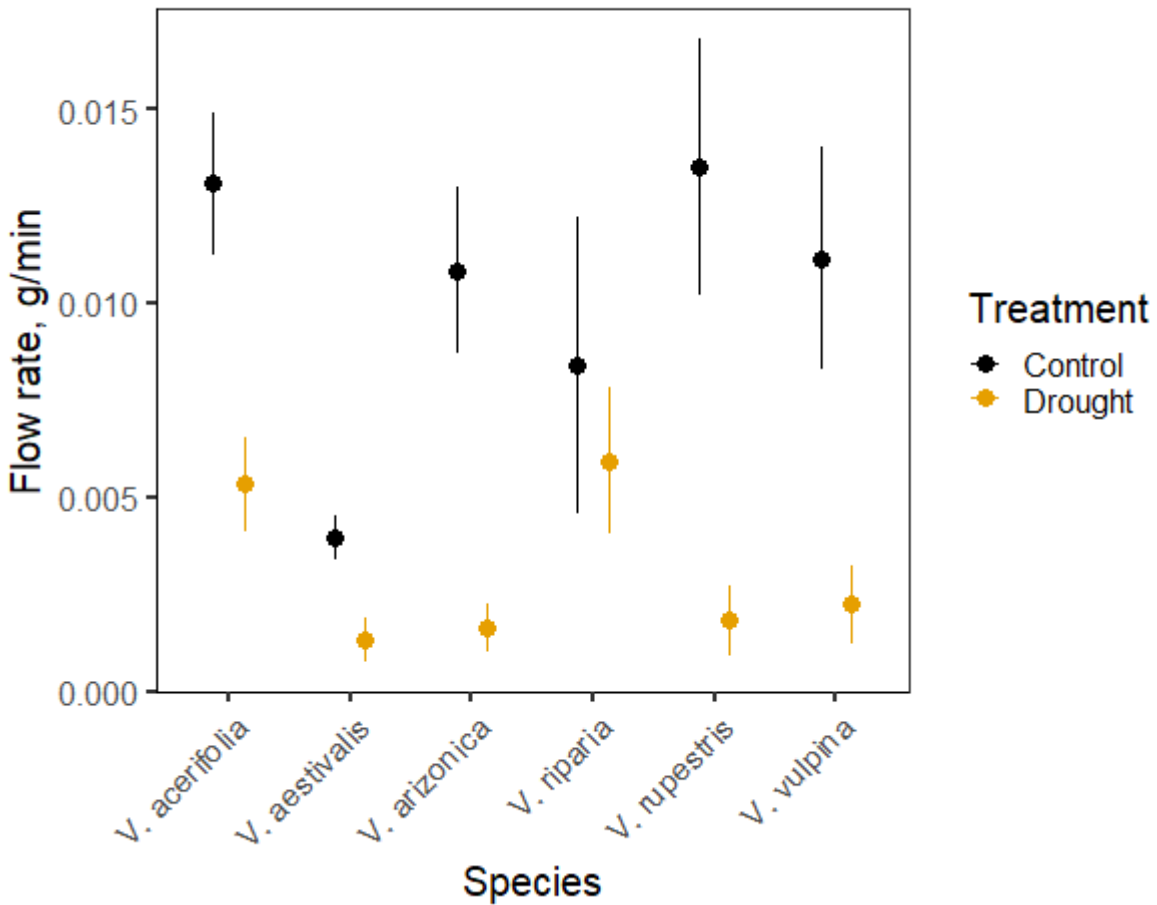
Figure 9. Root Exudate Flow Rate from 2019 Dry Down.
Root exudate flow rate was measured in 2019 potted grapevine experiment. Root exudate was collected from the stem after the canopy was excised and measured over 1 hour. Each point represents the mean of 4 or more grapevines. Bars represent standard error of the mean. Mean values and error bars correspond to data shown in Table 1. ANOVA results: Drought effect (F= 36.470, p=9.11e-08); Species effect (F=2.219, p=0.0632); Drought X Species effect (F=1.732, p=0.1402).
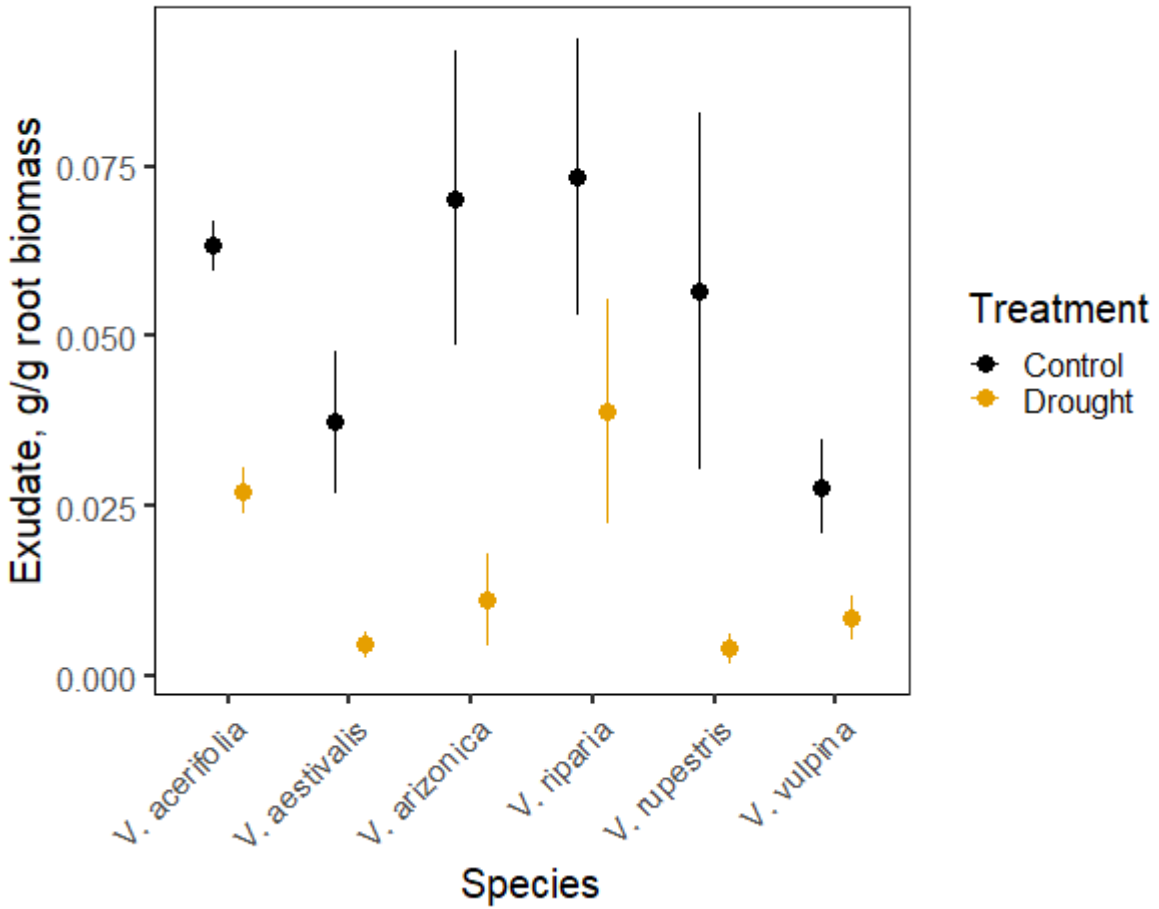
Figure 10. Root Exudate from 2019 Dry Down, Normalized for Root System Biomass.
Root exudate was collected in 2019 potted grapevine experiment at harvest and normalized
with dried root system biomass. Each point represents the mean of 4 or more grapevines. Bars
represent standard error of the mean. Mean values and error bars correspond to data shown in
Table 1.
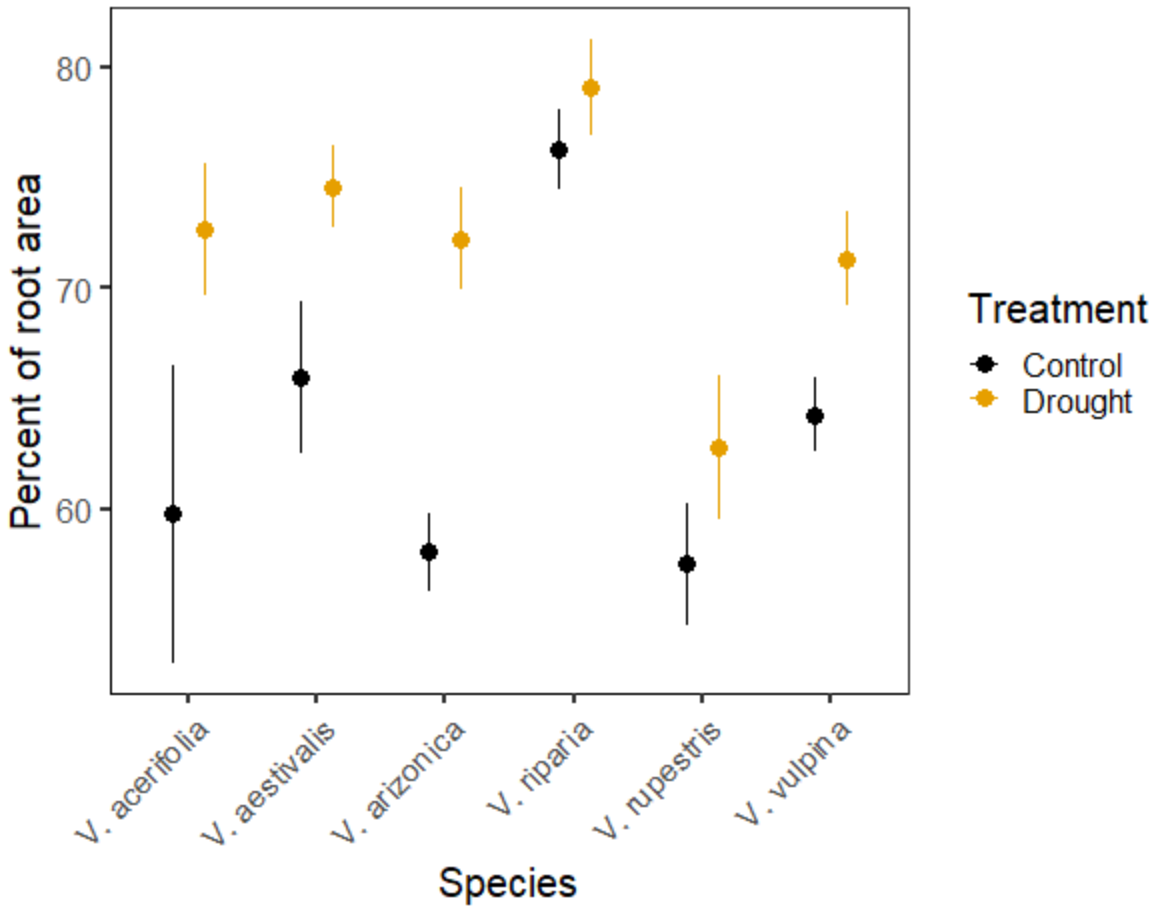
Figure 11. Suberized Regions of Root Systems from 2020 Dry Down.
Suberized regions of root systems were quantified by thresholding 300 dpi scanned images of individual roots that had been excised at the base of harvested root systems from 2020. Images were thresholded based on color to determine the percentage of brown (suberized) and white (unsuberized) regions of the roots, relative to total surface area. Each point represents the mean of 7 or more excised roots. Bars represent standard error of the mean. Mean values and error bars correspond to data shown in Table 3. ANOVA results: Drought effect (F= 20.001, p= 1.73e-05); Species effect (F= 7.003, p= .54e-06); Drought X Species effect (F= 0.896, p= 0.486).
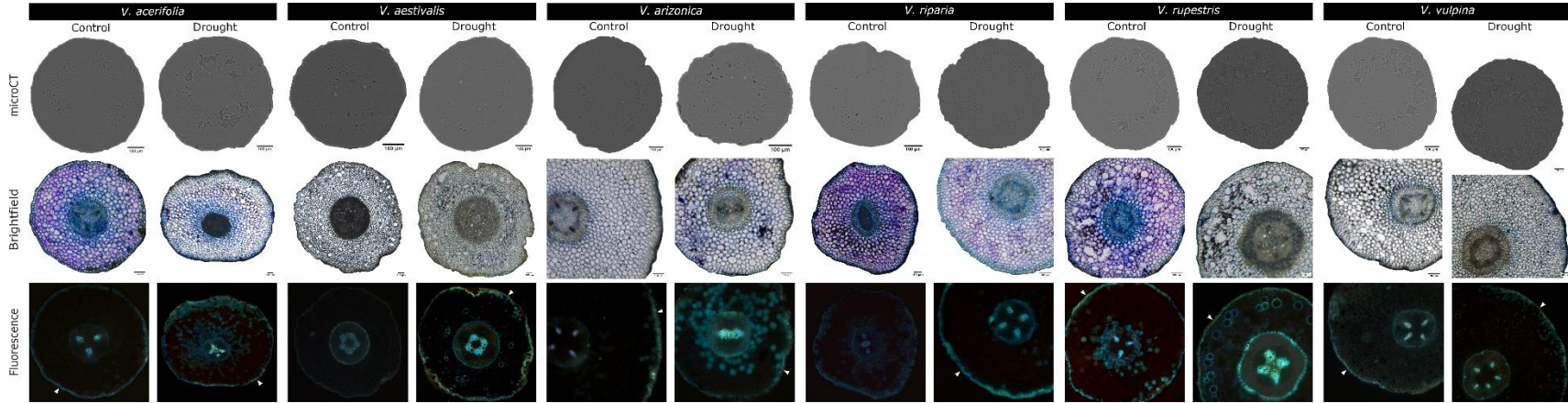
Root anatomy

Figure 12. Root Anatomical Features of *Vitis* spp. from 2020 Dry Down.
Transverse images were collected from 6-8 cm behind the root tip. MicroCT images of root segments were taken at Day 16 of experimental treatment. Target soil moisture for drought treatment on the day of microCT imaging was 30%. Microscope images were taken of hand-sectioned roots harvested at Day 42. Brightfield images show cell structure and fluorescence images show suberin-stained exodermis, indicated by arrows.
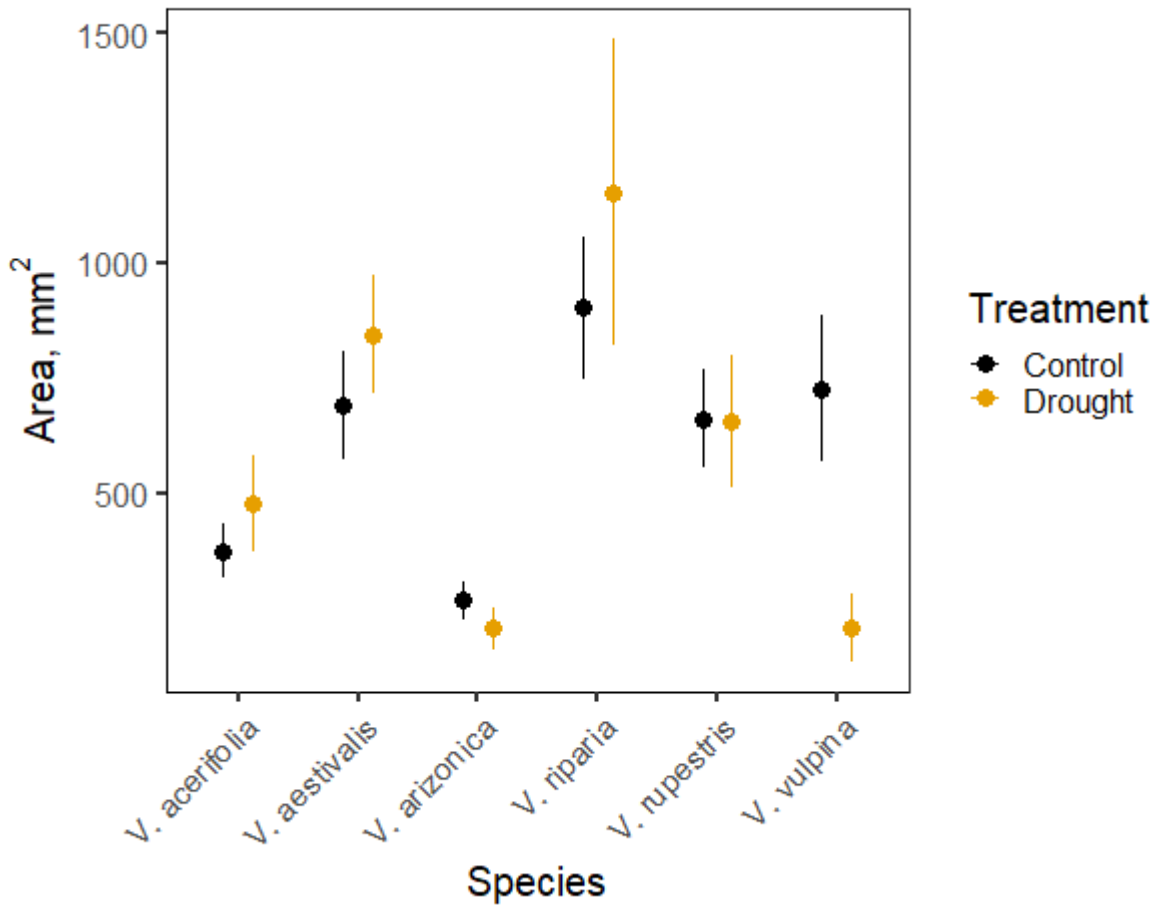
Figure 13. Cross-sectional Area of Excised Roots from 2020 Dry Down.
Cross-sectional area of excised roots was measured from microCT scans taken 6-8 cm back from root tip from 2020 dry down. Each point represents the mean of 4 or more excised roots. Bars represent standard error of the mean. Mean values and error bars correspond to data shown in Table 3. ANOVA results: Drought effect (F= 0.014, p= 0.907); Species effect (F= 6.385, p= 5.08e-05); Drought X Species effect (F= 1.494, p= 1.494).
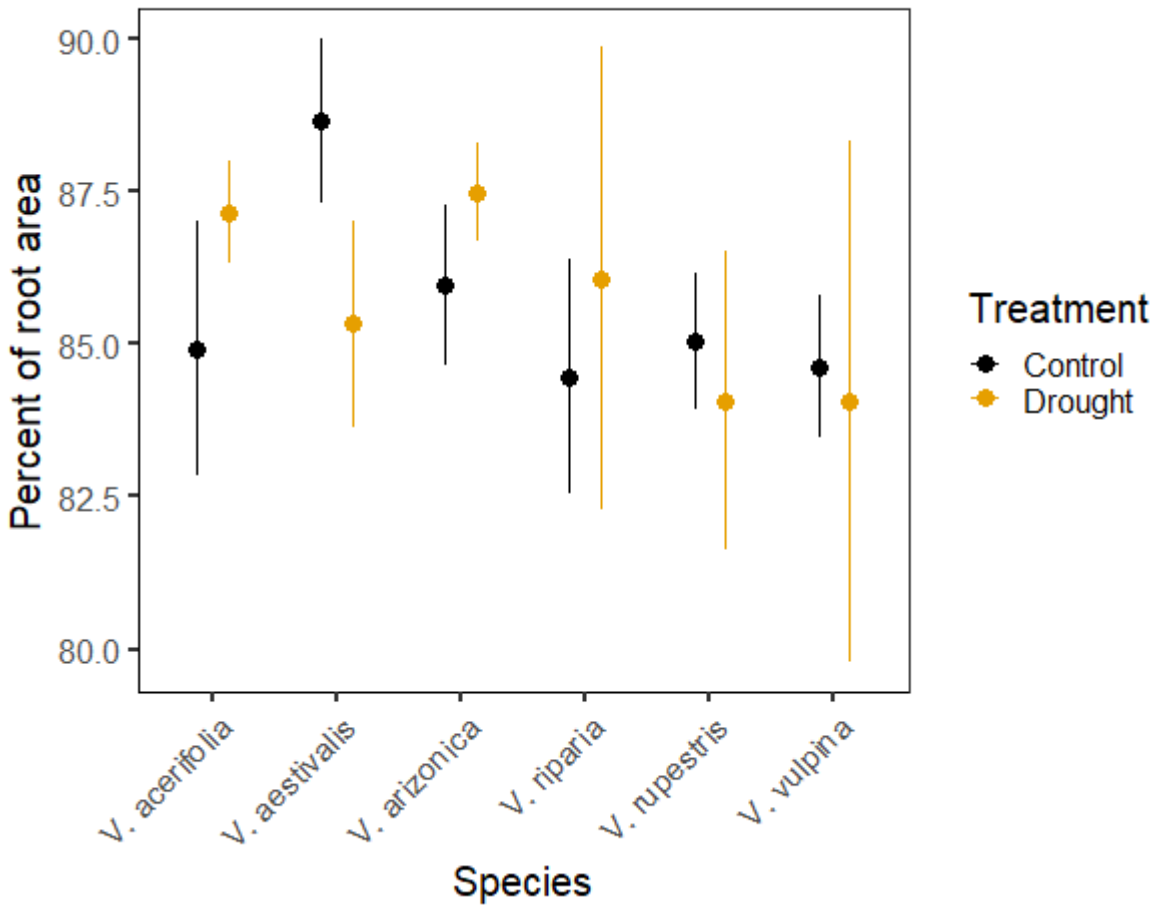
Figure 14. Root Cortex Area from 2020 Dry Down.
Area of root cortex was measured from microCT scans taken 6-8 cm back from root tip from 2020 dry down and reported as a percentage of cross-sectional root area. Each point represents the mean of 4 or more excised roots. Bars represent standard error of the mean. Mean values and error bars correspond to data shown in Table 3. No statistically significant differences were observed. ANOVA results: Drought effect (F= 0.180, p= 0.672); Species effect (F= 0.699, p= 0.626); Drought X Species effect (F= 0.727, p= 0.605).
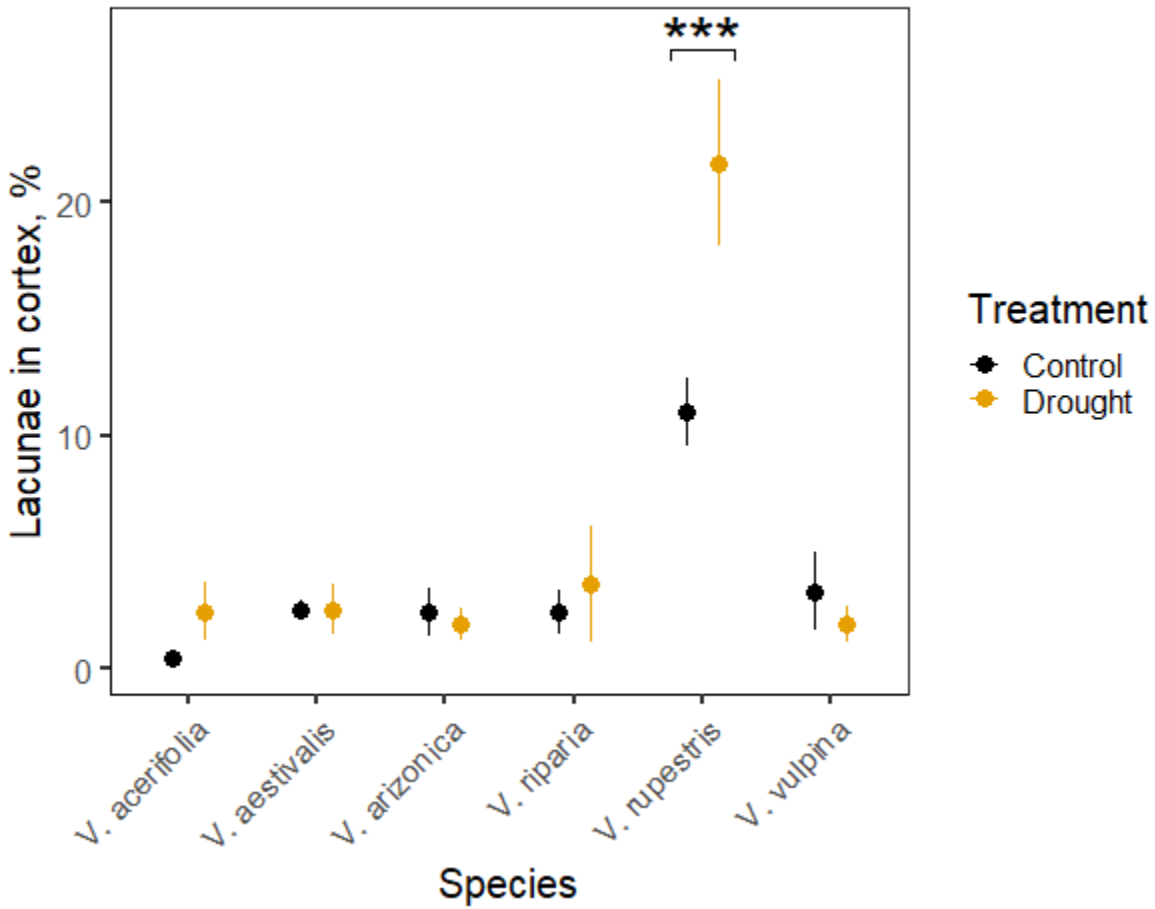
Figure 15. Lacuna in Root Cortex from 2019 Blotting Chambers and 2020 Dry Down. Lacuna was measured from microCT scans taken 6-8 cm back from root tip and reported as a percent of root cortex area. Each point represents the mean of 4 or more excised roots. Bars represent standard error of the mean. Mean values and error bars correspond to data shown in Table 3. ANOVA results: Drought effect (F= 4.566, p= 0.03633); Species effect (F= 25.221, p= 4e-14); Drought X Species effect (F= 4.568, p= 0.00123). Asterisks indicate post-hoc analysis, if statistically significant: ***p < .001.

Root architecture
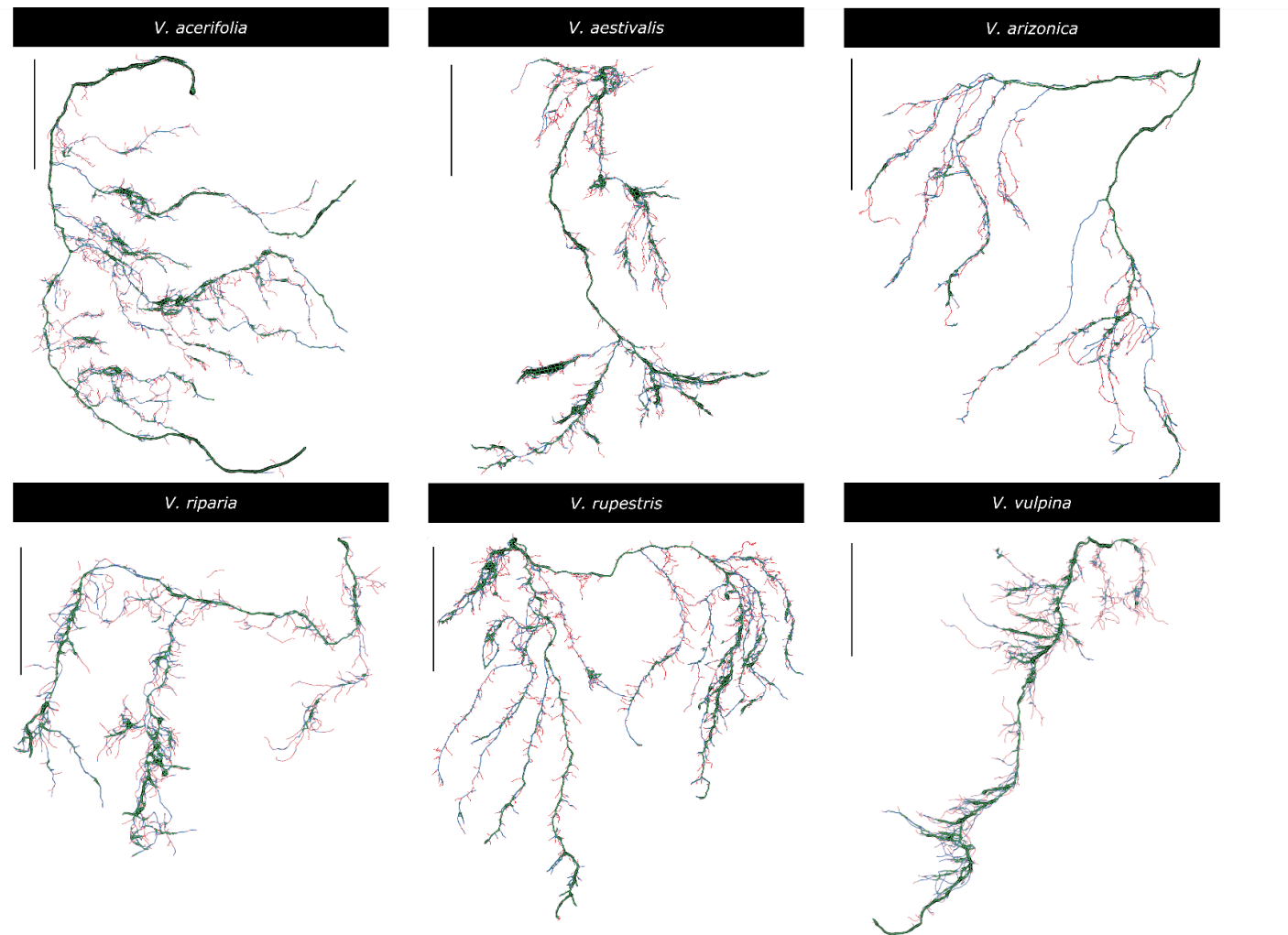
Figure 16. Scans of Excised Roots from 2020 Dry Down.
Excised roots were laid flat and scanned to produce binary images for analysis. Images are overlaid with colors to indicate root diameter ranges: 0-0.5 mm (red), 0.5-1 mm (blue), and >1 mm (green). Black scale bars represent 10 cm.
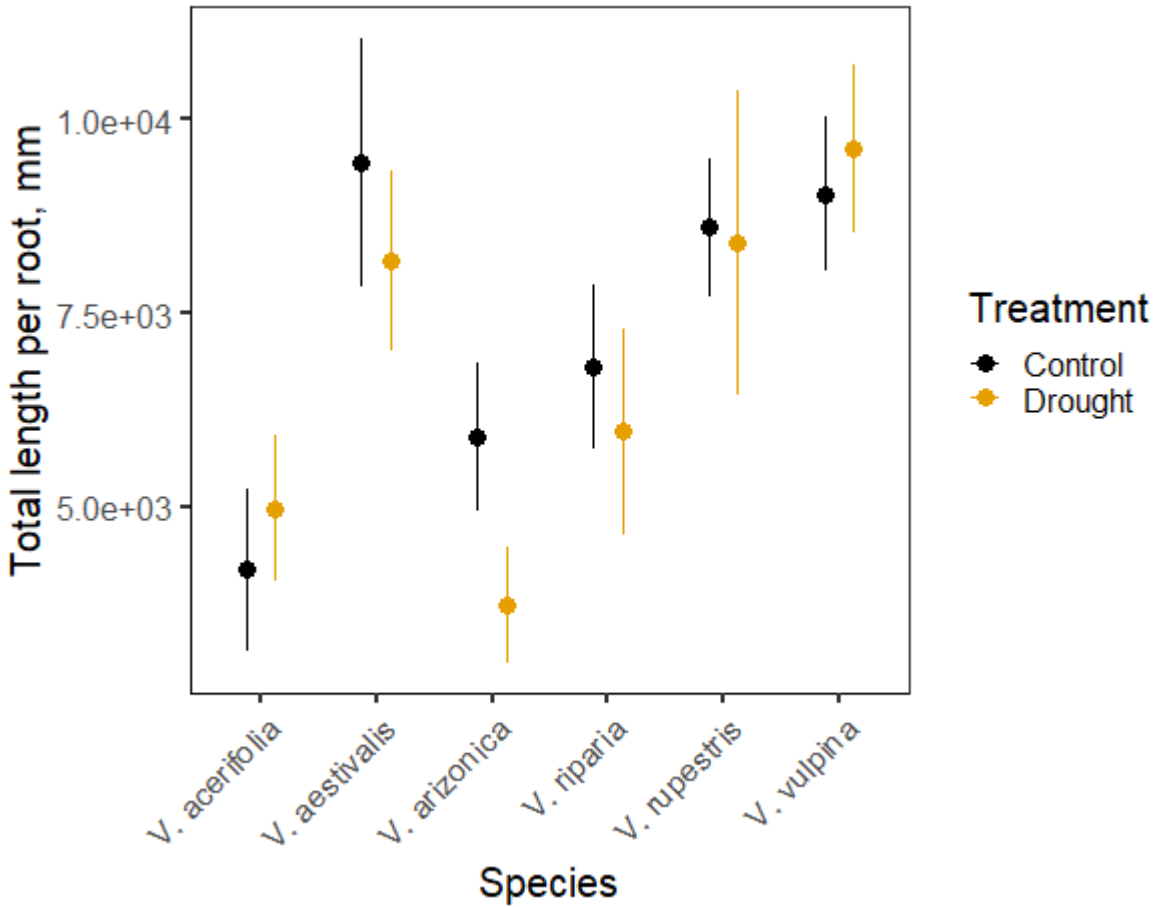
Figure 17. Total Root Length of Excised Roots from 2020 Dry Down.
Total root length of all root branches on excised roots from 2020 dry down was measured from binary masks with RhizoVision Explorer. Each point represents the mean of 8 or more excised roots. Bars represent standard error of the mean. Mean values and error bars correspond to data shown in Table 3. ANOVA results: Drought effect (F= 1.208, p= 0.274); Species effect (F= 5.859, p= 6.42e-05); Drought X Species effect (F= 0.868, p= 0.504).
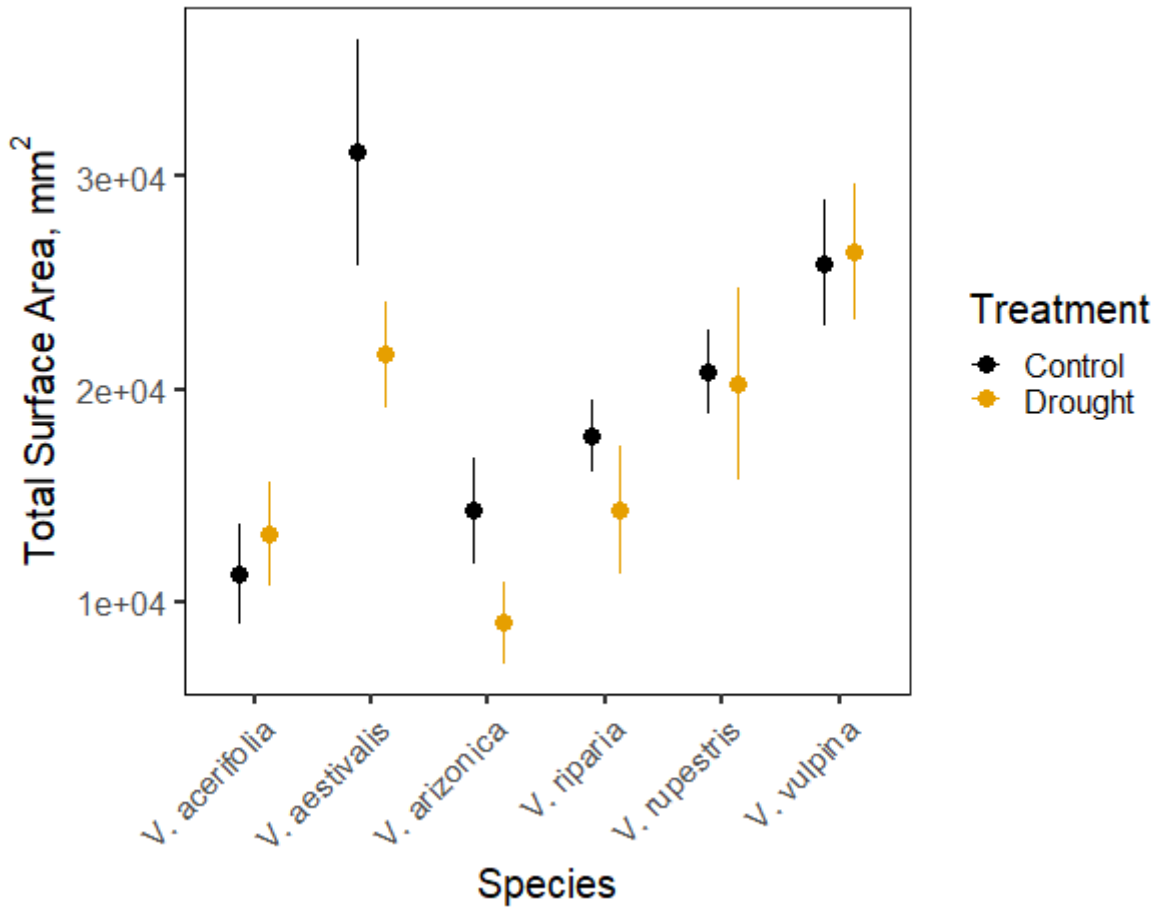
Figure 18. Total Surface Area of Excised Roots from 2020 Dry Down.
Total root surface area of all root branches on excised roots from 2020 dry down was measured from binary masks with RhizoVision Explorer. Each point represents the mean of 8 or more excised roots. Bars represent standard error of the mean. Mean values and error bars correspond to data shown in Table 3. ANOVA results: Drought effect (F= 2.598, p= 0.10943); Species effect (F= 4.320, p= 0.00114); Drought X Species effect (F= 0.681, p= 0.63890).
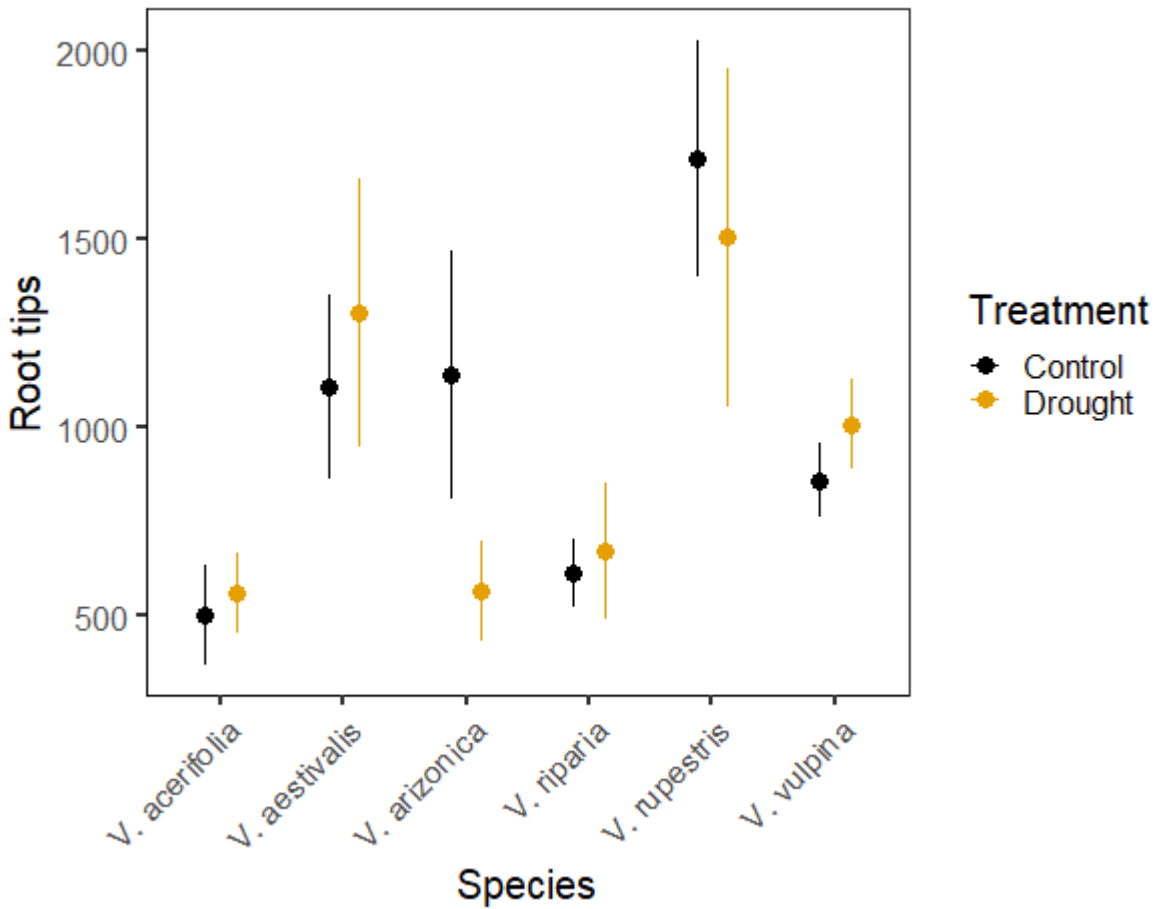
Figure 19. Root Tips of Excised Roots from 2020 Dry Down.
Individual roots were excised from 2020 dry down root systems, scanned and thresholded to create binary images, and analyzed with RhizoVision Explorer to count total number of tips per excised root. Each point represents the mean of 8 or more excised roots. Bars represent standard error of the mean. Mean values and error bars correspond to data shown in Table 3. ANOVA results: Drought effect (F= 0.054, p= 0.81687); Species effect (F= 5.067, p= 0.00028); Drought X Species effect (F= 0.683, p= 0.63685).
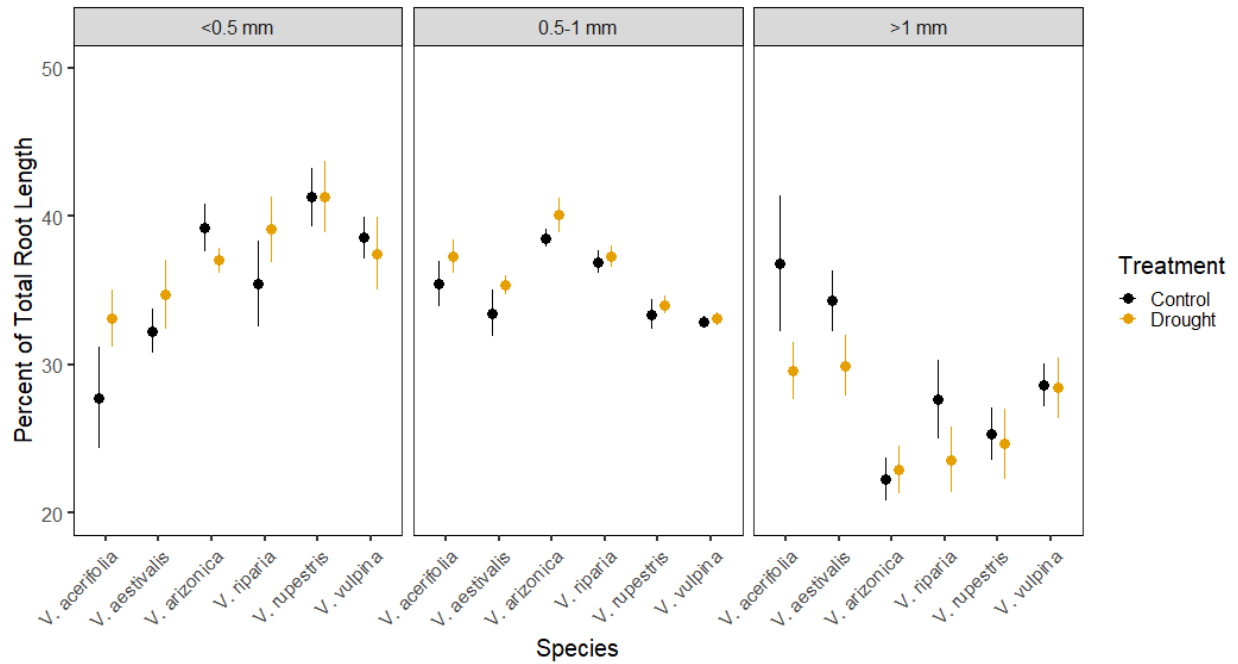
Figure 20. Root Length Grouped by Diameter.

Lengths of root branches were measured from binary images of excised roots from 2020 dry down, classified by diameter size, summed according to diameter class, and reported as a percent of total root length. Each point represents the mean of 8 or more excised roots. Bars represent standard error of the mean. Mean values and error bars correspond to data shown in Table 4. ANOVA results: Drought effect (F= 0.011, p= 0.9150); Species effect (F= 0.007, p= 1.0000); Order effect: (F= 68.003, p= < 2e-16); Drought X Species effect (F= 0.008, p= 1.0000), Drought X Order effect (F= 4.035, p= 0.0184); Species X Order effect: (F= 9.626, p= 2.14e-14); Drought X Species X Order effect (F= 1.236, p= 0.2659).
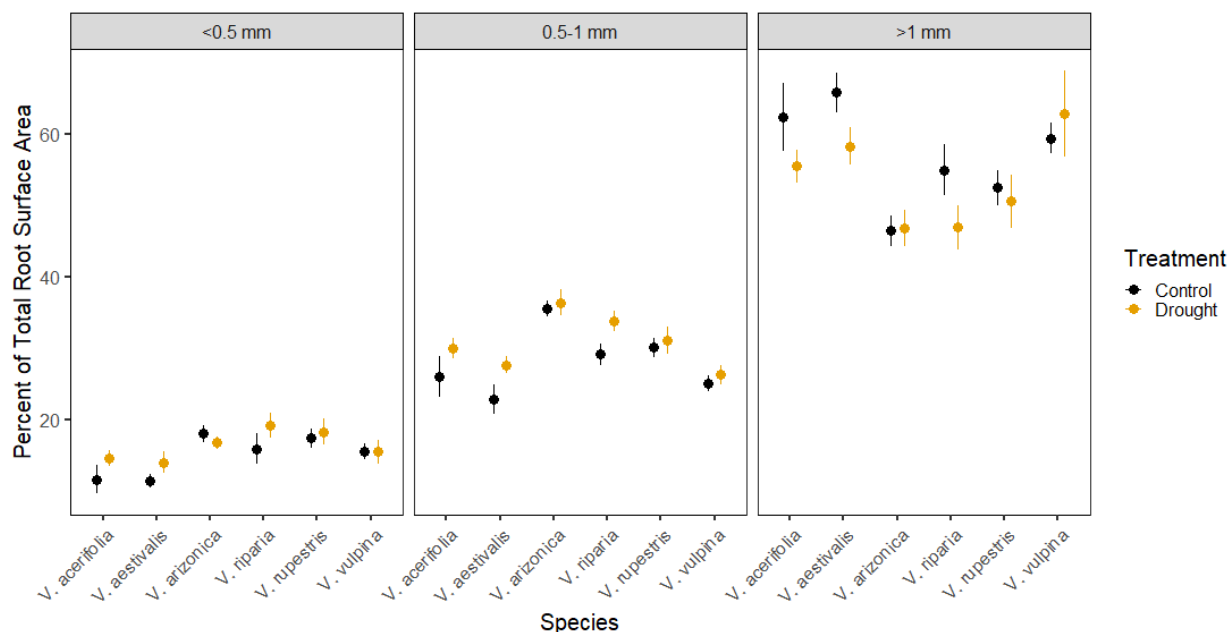
Figure 21. Root Surface Area Grouped by Diameter.
Root surface area was calculated using from lengths and diameters of root branches from binary images of excised roots, summed according to diameter class, and reported as a percent of total root surface area. Each point represents the mean of 8 or more excised roots. Bars represent standard error of the mean. Mean values and error bars correspond to data shown in Table 4. ANOVA results: Drought effect (F= 0.164, p= 0.68560); Species effect (F= 0.107, p= 0.99081); Order effect: (F= 827.107, p= < 2e-16); Drought X Species effect (F= 0.121, p= 0.98763), Drought X Order effect (F= 4.879, p= 0.00807); Species X Order effect: (F= 10.076, p= 4.09e-15); Drought X Species X Order effect (F= 1.262, p= 0.25019).
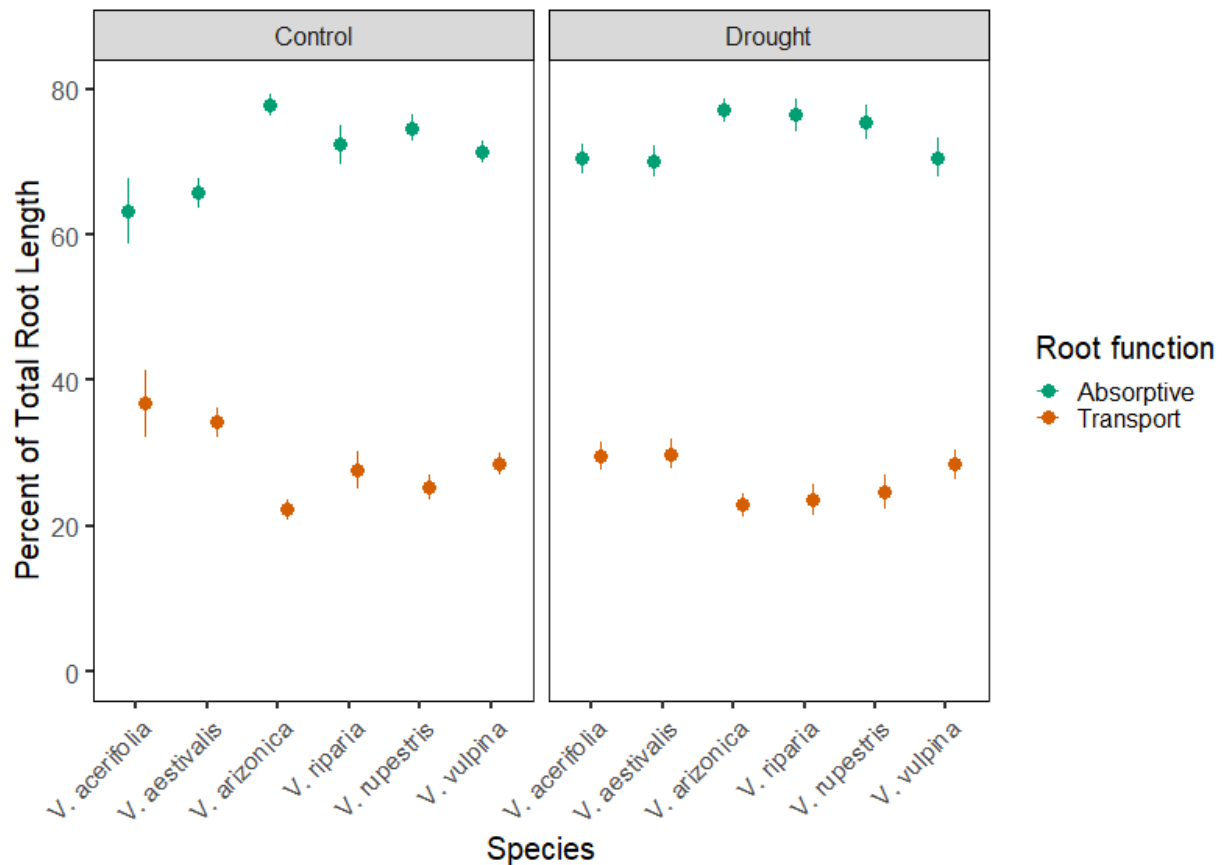
Figure 22. Root Length Grouped by Function.
Root Length was measured from binary masks of excised roots with RhizoVision Explorer and classified using root diameter size to assign functional class. Root lengths in each functional class were measured, summed, and reported as a percentage of total root length. Each point represents the mean of 8 or more excised roots. Bars represent standard error of the mean. Mean values and error bars correspond to data. ANOVA results: Drought effect (F=3.084, p= 0.0814); Species effect (F= 5.721, p= 8.3e-05); Drought X Species effect (F= 0.936, p= 0.4601).
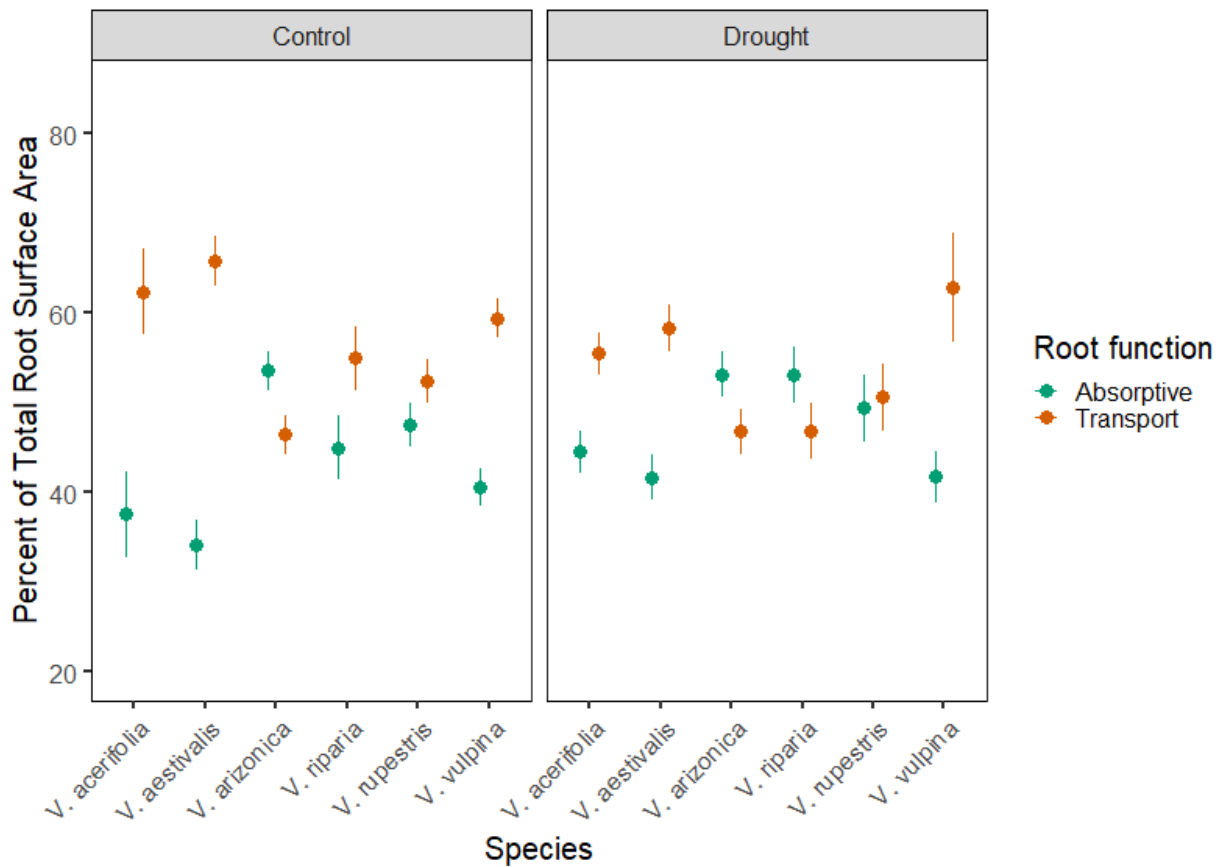
Figure 23. Root Surface Area By Function.
Root Length was measured from binary masks of excised roots with RhizoVision Explorer and classified using root diameter size to assign functional class. Root lengths in each functional class were measured, summed, and reported as a percentage of total root length. Each point represents the mean of 8 or more excised roots. Bars represent standard error of the mean. ANOVA results: Drought effect (F= 2.598, p= 0.10943); Species effect (F= 4.320, p= 0.00114); Drought X Species effect (F= 0.681, p= 0.63890).

Figure 24. Blotting Paper Chambers.
Blotting paper chambers for evaluating early-development root architecture and anatomy

Tables

Table 1. 2019 Dry Down Variables Measured at Harvest

Variable	*V. acerifolia*		*V. aestivalis*		*V. arizonica*	
	Control	Drought	Control	Drought	Control	Drought
Ψ_{PD}, bar	-3.39±0.64 ab	-6.95±1.09 ab	-2.32±0.44 b	-6.91±1.24 ab	-4.53±0.98 ab	-11±0.7 a
Ψ_{MD}, bar	-3.88±2.01 a	-6.34±3.47 a	-2.71±0.98 a	-10.51±1.92 a	-4.39±1.5 a	-7.99±3.31 a
Soil moisture, %	54±4 bc	5±6 a	70±3 c	4±3 a	56±7 bc	3±2 a
θ_{10cm}, %	21±3 abcdef	14±2 ab	27±3 ef	15±2 abc	25±2 def	10±1 a
θ_{25cm}, %	23±1 bcd	11±2 ab	32±4 cd	11±2 ab	18±5 abc	7±0 a
Root biomass, g	13.03±2.48 abc	11.61±2.08 ab	8.59±2.15 ab	15.33±1.77 abc	9.52±0.99 ab	13.66±2.11 abc
Canopy biomass, g	111.89±15.48 b	73.17±6.56 ab	69.14±9.17 ab	66.89±4.69 ab	102.32±16.82 ab	80.53±4.81 ab
Root:shoot ratio	0.11±0.01 ab	0.16±0.02 abc	0.12±0.02 abc	0.23±0.02 bc	0.12±0.04 ab	0.17±0.02 abc
Exudate flow, g/min	0.013±0.002 c	0.004±0.001 abc	0.011±0.002 bc	0.008±0.004 abc	0.014±0.003 c	0.011±0.003 bc
Exudate, g/g root biomass	0.063±0.004 abc	0.038±0.011 abc	0.082±0.022 c	0.074±0.02 bc	0.057±0.026 abc	0.028±0.007 abc

Variable	*V. riparia*		*V. rupestris*		*V. vulpina*	
	Control	Drought	Control	Drought	Control	Drought
Ψ_{PD}, bar	-2.2±0.19 b	-3.66±0.57 b	-3.55±0.39 b	-10.02±1.97 a	-3.43±0.21 b	-6.02±1.59 ab
Ψ_{MD}, bar	-3.97±1.38 a	-4.38±1.4 a	-3.87±1.2 a	-9.1±1.92 a	-4.76±1.25 a	-6.46±1.79 a
Soil moisture, %	68±5 c	27±15 ab	59±3 bc	4±6 a	53±8 bc	3±3 a
θ_{10cm}, %	24.83±1.8 cde	21.75±2.87 abcde	22.92±0.86 bcde	15.72±1.23 abc	29.85±3.66 e	15.8±3.7 abcd
θ_{25cm}, %	32.83±4.67 c	19±4.99 abc	19.22±3.31 abc	13.08±2.17 ab	24.27±1.97 bc	10.91±1.57 ab
Root biomass, g	6.22±2.01 a	10±2.53 ab	19.63±3.73 bc	17.8±3.88 abc	24.78±2.02 c	25.14±4.17 c
Canopy biomass, g	66.54±13.86 ab	55.86±8.11 a	103.78±9.32 ab	67.19±8.83 ab	86.41±5.19 ab	75.15±7.17 ab
Root:shoot ratio	0.08±0.02 a	0.19±0.07 abc	0.19±0.02 abc	0.26±0.03 cd	0.26±0.02 bcd	0.35±0.02 d
Exudate flow, g/min	0.005±0.001 abc	0.001±0.001 a	0.002±0.001 ab	0.006±0.002 abc	0.002±0.001 ab	0.002±0.001 ab
Exudate, g/g root biomass	0.027±0.003 abc	0.005±0.002 a	0.011±0.007 ab	0.039±0.017 abc	0.004±0.002 a	0.009±0.003 a

Values are given as mean ± SE (n = 4-8 grapevines). For a given variable, different letters indicate statistically significant differences among means ($p < 0.05$).

Table 2. 2020 Dry Down Variables Measured at Harvest

Variable	V. acerifolia		V. aestivalis		V. arizonica	
	Control	Drought	Control	Drought	Control	Drought
Ψ_{PD}, bar	-7.42±0.65 ab	-7.08±0.49 ab	-6.94±0.97 b	-7.73±1.07 ab	-8.02±0.9 ab	-13.62±3.76 a
Ψ_{MD}, bar	-10.92±1.27 ab	-12±1.29 ab	-9.53±1.13 ab	-11.76±1.31 ab	-11.58±1.44 ab	-14.74±1.06 a
Soil moisture, %	76±2 b	20±1 a	73±2 b	23±1 a	76±4 b	27±4 a
θ_{10cm}, %	37±4 cde	20±3 abc	34±4 abcde	23±4 abcd	27±2 abcd	15±4 a
θ_{25cm}, %	47±4 de	18±3 ab	44±3 cde	21±11 abc	38±2 bcde	9±1 a
Root biomass, g	17.71±3.48 abc	15.38±2.43 abc	23.07±2.79 c	17.94±2.6 abc	11.66±0.97 ab	7.23±0.88 a
Canopy biomass, g	61.52±8.91 b	16.28±4.24 a	54.26±5.21 b	9.42±1.93 a	102.72±4.12 c	23.76±2.8 a
Root:shoot	0.3±0.02 a	1.16±0.24 ab	0.43±0.06 a	1.88±0.43 bc	0.11±0.01 a	0.32±0.05 a
Stem diameter, mm	7.05±0.29 e	6±0.44 cde	6.04±0.1 cde	4.05±0.23 a	6.85±0.21 de	5.09±0.08 abc

Variable	V. riparia		V. rupestris		V. vulpina	
	Control	Drought	Control	Drought	Control	Drought
Ψ_{PD}, bar	-7.28±1.12 ab	-5.74±0.74 b	-6.8±0.85 b	-8.2±0.89 ab	-7.5±0.67 ab	-8.58±0.72 ab
Ψ_{MD}, bar	-9.54±1.25 ab	-8.1±1.35 b	-13.18±1.29 ab	-12.76±1.41 ab	-12.6±1.75 ab	-11.72±1.47 ab
Soil moisture, %	77±1 b	19±2 a	76±3 b	20±1 a	81±2 b	25±3 a
θ_{10cm}, %	49±5 e	20±4 abc	36±6 bcde	21±5 abc	45±3 de	15±4 ab
θ_{25cm}, %	57±4 e	25±7 abcd	48±3 de	9±1 a	62±7 e	22±5 abc
Root biomass, g	14.75±1.85 abc	10.73±1.07 ab	21.07±1.69 bc	16.82±0.29 abc	17.4±2.36 abc	17.03±3.06 abc
Canopy biomass, g	50.06±2.69 b	19.3±1.9 a	52.25±8.83 b	13.8±1.46 a	22.4±4.09 a	7.12±2.5 a
Root:shoot	0.29±0.02 a	0.56±0.04 ab	0.59±0.22 ab	1.16±0.1 ab	0.83±0.11 ab	2.97±0.7 c
Stem diameter, mm	5.69±0.12 bcd	5.01±0.38 abc	6.99±0.43 de	4.76±0.22 abc	4.64±0.41 abc	4.49±0.38 ab

Values are given as mean ± SE (n = 4-8 grapevines). For a given variable, different letters indicate statistically significant differences among means ($p < 0.05$).

Table 3. Root Anatomy & Hydraulic Features

Variable	*V. acerifolia*				*V. aestivalis*				*V. arizonica*			
	Control		Drought		Control		Drought		Control		Drought	
Root cross-sectional area, mm^2	372.36±58.84	abc	475.92±106.29	abc	689.98±116.78	abc	842.96±128.99	bc	265.52±41.35	a	204.55±45.3	ab
Cortex, % of root area	84.93±2.09	a	87.16±0.84	a	88.66±1.35	a	85.34±1.69	a	85.97±1.31	a	87.49±0.81	a
Lacuna, % of root area	0.48±0.25	a	2.43±1.24	a	2.55±0.4	a	2.53±1.06	a	2.41±1.05	a	1.93±0.68	a
Suberization, % of root area	40.23±6.71	cd	27.08±2.75	abc	34.05±3.4	abcd	25.41±1.88	ab	41.96±1.74	d	27.76±2.27	abcd
Total root length, mm	4194.29±1043.4	a	4983.54±952.6	ab	9454.87±1602.31	ab	8168.95±1164.61	ab	5902.49±959.23	ab	3744.31±748.76	ab
Total root surface area, mm^2	11298.87±2356.94	a	13195.72±2446.35	a	31167.11±5329.44	c	21645.47±2495.69	abc	14298.43±2498.74	ab	9002.01±1899.19	a
Root tips	502±131	a	562±106	ab	1107±243	ab	1305±359	ab	1140±332	ab	566±131	ab

Variable	*V. riparia*				*V. rupestris*				*V. vulpina*			
	Control		Drought		Control		Drought		Control		Drought	
Root cross-sectional area, mm^2	903±154.76	bc	1153.31±333.88	c	660.82±107.54	abc	656.49±143.49	abc	725.1±159.02	abc	204.96±73.36	ab
Cortex, % of root area	84.47±1.92	a	86.08±3.81	a	85.05±1.12	a	84.08±2.45	a	84.63±1.16	a	84.07±4.28	a
Lacuna, % of root area	2.39±0.94	a	3.59±2.49	a	11.03±1.47	b	21.68±3.54	c	3.32±1.68	a	1.88±0.77	a
Suberization, % of root area	23.73±1.79	ab	20.91±2.18	a	42.5±2.75	d	37.22±3.24	bcd	35.81±1.56	bcd	27.63±1.62	abcd
Total root length, mm	6806.73±1054.95	ab	5970.32±1326.45	ab	8607.89±890.12	ab	8404.59±1957	ab	9037.41±1001.33	ab	9617.09±1080.35	b
Total root surface area, mm^2	17812.61±1725.51	abc	14320.34±2983.08	ab	20797.27±2005.8	abc	20257.05±4528.07	abc	25942.32±2930.07	bc	26476.39±3184.34	bc
Root tips	614±89	ab	672±179	ab	1717±315	b	1506±449	ab	860±98	ab	1008±120	ab

Values are given as mean ± SE (n = 4-8 grapevines). For a given variable, different letters indicate statistically significant differences among means ($p < 0.05$).

Table 4. Root Architecture by Size Class

V. acerifolia

Root size class	Control			Drought		
	<0.5 mm	0.5-1 mm	>1 mm	<0.5 mm	0.5-1 mm	>1 mm
Root length, % of excised root	27.77±3.42 [abcdef]	35.42±1.54 [efghij]	36.81±4.57 [fghij]	33.12±1.89 [bcdefghij]	37.3±1.15 [fghij]	29.58±1.96 [abcdefgh]
Root surface area, % of excised root	11.61±2.01 [a]	25.98±2.83 [bcdef]	62.41±4.79 [lm]	14.58±1.18 [ab]	29.93±1.44 [ef]	55.48±2.3 [jklm]

V. aestivalis

Root size class	Control			Drought		
	<0.5 mm	0.5-1 mm	>1 mm	<0.5 mm	0.5-1 mm	>1 mm
Root length, % of excised root	32.25±1.49 [abcdefghij]	33.44±1.57 [bcdefghij]	34.31±2.05 [bcdefghij]	34.71±2.34 [cdefghij]	35.35±0.65 [defghij]	29.94±2.07 [abcdefghi]
Root surface area, % of excised root	11.36±0.97 [a]	22.83±2.09 [abcdef]	65.81±2.83 [m]	14.01±1.47 [ab]	27.68±1.23 [cdef]	58.3±2.57 [jklm]

V. arizonica

Root size class	Control			Drought		
	<0.5 mm	0.5-1 mm	>1 mm	<0.5 mm	0.5-1 mm	>1 mm
Root length, % of excised root	39.24±1.6 [hij]	38.51±0.62 [hij]	22.25±1.44 [a]	37.01±0.81 [efghij]	40.06±1.16 [ghij]	22.93±1.63 [abc]
Root surface area, % of excised root	18.02±1.2 [abcde]	35.55±1.09 [fgh]	46.42±2.16 [hij]	16.78±0.85 [abcde]	36.41±1.79 [fghi]	46.81±2.5 [ghijk]

V. riparia

Root size class	Control			Drought		
	<0.5 mm	0.5-1 mm	>1 mm	<0.5 mm	0.5-1 mm	>1 mm
Root length, % of excised root	35.43±2.92 [defghij]	36.91±0.79 [efghij]	27.65±2.62 [abcdefg]	39.1±2.21 [hij]	37.3±0.75 [fghij]	23.6±2.2 [ab]
Root surface area, % of excised root	15.9±2.14 [abcd]	29.12±1.57 [def]	54.98±3.57 [jklm]	19.26±1.76 [abcde]	33.83±1.48 [fg]	46.91±3.13 [hij]

V. rupestris

Root size class	Control			Drought		
	<0.5 mm	0.5-1 mm	>1 mm	<0.5 mm	0.5-1 mm	>1 mm
Root length, % of excised root	41.27±1.96 [ij]	33.38±1 [abcdefghij]	25.35±1.76 [abcde]	41.31±2.41 [j]	34.03±0.62 [bcdefghij]	24.66±2.35 [abcd]
Root surface area, % of excised root	17.39±1.32 [abcde]	30.14±1.35 [def]	52.47±2.45 [jklm]	18.3±1.86 [abcde]	31.09±1.93 [ef]	50.61±3.73 [ijkl]

V. vulpina

Root size class	Control			Drought		
	<0.5 mm	0.5-1 mm	>1 mm	<0.5 mm	0.5-1 mm	>1 mm
Root length, % of excised root	38.53±1.39 [hij]	32.87±0.39 [bcdefghij]	28.6±1.46 [abcdef]	37.48±2.48 [fghij]	33.08±0.42 [bcdefghij]	28.45±2.05 [abcdef]
Root surface area, % of excised root	15.49±1.09 [abc]	25.08±1.08 [bcdef]	59.43±2.14 [klm]	15.52±1.69 [abc]	26.28±1.36 [bcdef]	62.87±6.08 [lm]

Values are given as mean ± SE (n = 8-16 excised roots). For a given variable, different letters indicate statistically significant differences among means (p < 0.05).

References

Alsina, M. M., Smart, D., Bauerle, T., De Herralde, F., Biel, C., Stockert, C., . . . Save, R. (2011). Seasonal changes of whole root system conductance by a drought-tolerant grape root system. *Journal of Experimental Bbotany, 62*, 99-109.

Aroca, R., Porcel, R., & Ruiz-Lozano, J. M. (2012). Regulation of root water uptake under abiotic stress conditions. *Journal of Experimental Botany, 63*, 43-57.

Barrios-Masias, F., Knipfer, T., & McElrone, A. J. (2015). Differential responses of grapevine rootstocks to water stress are associated with adjustments in fine root hydraulic physiology and suberization. *Journal of Experimental Botany, 66*, 6069–6078.

Barrios-Masias, F., Knipfer, T., Walker, M. A., & McElrone, A. J. (2019). Differences in hydraulic traits of grapevine rootstocks are not conferred to a common Vitis vinifera scion. *Functional Plant Biology, 46*, 228-235.

Blum, A. (2011). Plant Water Relations, Plant Stress and Plant Production. In *Plant Breeding for Water-Limited Environments.* New York, NY: Springer.

Blum, A. (2015). Towards a conceptual ABA ideotype in plant breeding for water limited environments. *Functional Plant Biology, 42*, 502-513.

Bodner, G., Nakhforoosh, A., & Kaul, H. (2015). Management of crop water under drought: a review. *Agronomy for Sustainable Development, 35*, 401-442.

Cardoso, A. A., Visel, D., Kane, C. N., Batz, T. A., García Sánchez, C., Kaack, L., . . . Corso, D. (2020). Drought-induced lacuna formation in the stem causes hydraulic conductance to decline before xylem embolism in Selaginella. *New Phytologist, 227*, 1804-1817.

Comas, L., Becker, S., Cruz, V., Byrne, P., & Dierig, D. (2013). Root traits contributing to plant productivity under drought. *Frontiers in Plant Science, 4*, 442.

Condon, A. G., Richards, R. A., Rebetzke, G. J., & Farquhar, G. D. (2002). Improving intrinsic water-use efficiency and crop yield. *Crop Science, 42*, 122-131.

Cook, E. R., Woodhouse, C. A., Eakin, C. M., Meko, D. M., & Stahle, D. W. (2004). Long-term aridity changes in the western United States. *Science, 306*, 1015-1018.

Cuneo, I. F., Barrios-Masias, F., Knipfer, T., Uretsky, J., Reyes, C., Lenain, P., . . . McElrone, A. J. (2021). Differences in grapevine rootstock sensitivity and recovery from drought are linked to fine root cortical lacunae and root tip function. *New Phytologist, 229*, 272-283.

Cuneo, I. F., Knipfer, T., Brodersen, C. R., & McElrone, A. J. (2016). Mechanical failure of fine root cortical cells initiates plant hydraulic decline during drought. *Plant Physiology, 172*, 1669–1678.

Fort, K., Fraga, J., Grossi, D., & Walker, M. A. (2017). Early measures of drought tolerance in four grape rootstocks. *Journal of the American Society for Horticultural Science, 142*, 36-46.

Gambetta, G. A., Fei, J., Rost, T., Knipfer, T., Matthews, M., Shackel, K., . . . McElrone, A. J. (2013). Water uptake along the length of grapevine fine roots: developmental anatomy, tissue-specific aquaporin expression, and pathways of water transport. *Plant Physiology, 163*, 1254–1265.

Gambetta, G. A., Manuck, C. M., Drucker, S. T., Shaghasi, T., Fort, K., Matthews, M. A., . . . McElrone, A. J. (2012). The relationship between root hydraulics and scion vigour across Vitis rootstocks: what role do root aquaporins play? *Journal of Experimental Botany, 63*, 6445-6455.

Hachez, C., Veselov, D., Ye, Q., Reinhardt, H., Knipfer, T., Fricke, W., & Chaumont, F. (2012). Short-term control of maize cell and root water permeability through plasma membrane aquaporin isoforms. *Plant, Cell & Environment, 35*, 185-198.

Ho, M., Rosas, J., Brown, K., & Lynch, J. (2005). Root architectural tradeoffs for water and phosphorus acquisition. *Functional Plant Biology, 32*, 737-748.

Huang, B., & Eissenstat, D. (2000). Linking hydraulic conductivity to anatomy in plants that vary in specific root length. *Journal of the American Society for Horticultural Science, 125*, 260–264.

Knipfer, T., & Fricke, W. (2011). Water uptake by seminal and adventitious roots in relation to whole-plant water flow in barley (Hordeum vulgare L.). *Journal of Experimental Botany, 62*, 717-733.

Knipfer, T., Reyes, C., Earles, J., Berry, Z., Johnson, D., Brodersen, C., & McElrone, A. (2019). Spatiotemporal coupling of vessel cavitation and discharge of stored xylem water in a tree sapling. *Plant Physiology, 179*, 1658–1668.

Knipfer, T., Reyes, C., Momayyezi, M., Brown, P. J., Kluepfel, D., & McElrone, A. J. (2020). A comparative study on physiological responses to drought in walnut genotypes (RX1, Vlach, VX211) commercially available as rootstocks. *Trees, 52*, 1-14.

Kramer, P. J., & Boyer, J. S. (1995). *Water Relations of Plants and Soils.* Academic Press.

Lavely, E. K., Chen, W., Peterson, K. A., Klodd, A. E., Volder, A., Marini, R. P., & Eissenstat, D. M. (2020). On characterizing root function in perennial horticultural crops. *American Journal of Botany, 107*, 1214-1224.

Levin, A. D., Williams, L. E., & Matthews, M. A. (2020). A continuum of stomatal responses to water deficits among 17 wine grape cultivars (Vitis vinifera). *Functional Plant Biology, 47*, 11-25.

Lovisolo, C., Perrone, I., Carra, A., Ferrandino, A., Flexas, J., Medrano, H., & Schubert, A. (2010). Drought-induced changes in development and function of grapevine (Vitis spp.) organs and in their hydraulic and non-hydraulic interactions at the whole-plant level: a physiological and molecular update. *Functional Plant Biology, 37*, 98-116.

McCormack, M. L., Dickie, I. A., Fahey, T. J., Fernandez, C. W., Guo, D., Helmisaari, H. S., . . . Leppälammi-Kujansuu, J. (2015). Redefining fine roots improves understanding of below-ground contributions to terrestrial biosphere processes. *New Phytologist, 207*, 505-518.

Nobel, P. S., & Cui, M. (1992). Hydraulic conductances of the soil, the root-soil air gap, and the root: changes for desert succulents in drying soil. *Journal of Experimental Botany, 43*, 319-326.

North, G. B., & Nobel, P. S. (1991). Changes in hydraulic conductivity and anatomy caused by drying and rewetting roots of Agave deserti (Agavaceae). *American Journal of Botany, 78*, 906-915.

Padgett-Johnson, M., Williams, L. E., & Walker, M. A. (2003). Vine water relations, gas exchange, and vegetative growth of seventeen Vitis species grown under irrigated and nonirrigated conditions in California. *Journal of the American Society for Horticultural Science, 128*, 269–276.

Queen, A. (1967). Kinetics of the hydrolysis of acyl chlorides in pure water. *Canadian Journal of Chemistry, 45*, 1619-1629.

Rieger, M., & Litvin, P. (1999). Root system hydraulic conductivity in species with contrasting root anatomy. *Journal of Experimental Botany, 50*, 201-209.

RStudio Team. (2020). RStudio: Integrated Development for R. RStudio. Boston, MA: PBC. Retrieved from http://www.rstudio.com/

Seethepalli, A., & York, L. (2020). RhizoVision Explorer - Interactive software for generalized root image analysis designed for everyone. *Zenodo*. doi:http://doi.org/10.5281/zenodo.4095629

Skelton, R. (2020). Stem diameter fluctuations provide a new window into plant water status and function. *Plant Physiology, 183*, 1414–1415.

Steudle, E. (2000). Water uptake by roots: effects of water deficit. *Journal of Experimental Botany, 51*, 1531-1542.

Steudle, E., & Peterson, C. A. (1998). How does water get through roots? *Journal of Experimental Botany, 49*, 775-788.

Yang, X., Li, Y., Ren, B., Ding, L., Gao, C., Shen, Q., & Guo, S. (2012). Drought-induced root aerenchyma formation restricts water uptake in rice seedlings supplied with nitrate. *Plant and Cell Physiology, 53*, 495-504.

Zhu, J., Brown, K. M., & Lynch, J. P. (2010). Root cortical aerenchyma improves the drought tolerance of maize (Zea mays L.). *Plant, Cell & Environment, 33*, 740-749.